



Application of Nanomaterials in Food Quality Assessment

1

Milad Torabfam, Qandeel Saleem, Prabir Kumar Kulabhusan, Mustafa Kemal Bayazit, and Meral Yüce

Abstract

The food industry has a significant role to play in governing local economies all over the world. This sector includes some processes such as storage of raw materials, food production, and preservation. Food processing, food quality, and safety are vital to protect public health. Thus, food safety monitoring, for example, early detection of food pathogens, food-related toxins, allergens, chemicals, and enterotoxins, is of great significance. Nanoscience-based sensing platforms have become alternatives to conventional food safety monitoring techniques. Over the past few years, scientists have designed various novel nanosensors with high sensitivity and selectivity to detect a wide variety of hazardous substances. The nanomaterials, such as carbon-based nanoparticles, plasmonic/metallic nanoparticles, and inorganic fluorescent nanomaterials, have been extensively used to develop various detection platforms over the past few decades. The surface functionalization of nanoparticles using target-specific biological agents, such as aptamers and antibodies, has contributed to improving the efficiency of those nanoparticle-based diagnostic tools. In this chapter, general structural, physicochemical, and optical features of the nanoparticles were described, and their applications in food safety monitoring were reviewed. Following this, affinity agents and fundamental sensing principles employed in developing food-related hazardous substance detection tools were elaborated

M. Torabfam · Q. Saleem
Sabanci University, Faculty of Engineering and Natural Sciences, Istanbul, Turkey

P. K. Kulabhusan
The Institute for Global Food Security, Queen's University, Belfast, UK

M. K. Bayazit · M. Yüce (✉)
SUNUM Nanotechnology Research and Application Centre, Sabanci University, Istanbul, Turkey
e-mail: meralyuce@sabanciuniv.edu

© The Author(s), under exclusive licence to Springer Nature Singapore Pte Ltd. 2022

P. Chandra, P. S. Panesar (eds.), *Nanosensing and Bioanalytical Technologies in Food Quality Control*, https://doi.org/10.1007/978-981-16-7029-9_1

1

based on the recent publications in the literature. Finally, we expect to pave the way for enhancing the efficiency and applicability of nanosensors in the initial sensing of food-related targets that cause a significant risk for humankind worldwide.

Keywords

Nanoparticles · Aptamers · Monoclonal antibodies · Food safety · Biosensors · Toxins · Allergens · Pathogens · Enterotoxins

1.1 Introduction

Human health and well-being largely depend on the quality of food that we consume. The simple yet essential idea of “you are what you eat” is well-acknowledged and adequately established. However, environmental degradation caused by rapid industrialization, infiltration of hazardous chemical and biological contaminants into food through soil and water, novel foodborne diseases and health complications, and swiftly changing eating habits have made food quality assessment and safety more critical now than ever (Pan et al. 2019). Moreover, the advances in the food and agriculture industry, stringent guidelines set by global regulatory agencies, and the growing competition between local catering businesses as well as international food supply chains have also made food quality assurance inevitable.

Food quality assessment encompasses the identification and quantification of food contaminants like colorants and additives, chemicals, toxins and enterotoxins, allergens, pathogens, heavy metal ions, residual pesticides, and other pollutants. In a typical food production process, quality control is often performed at the end with one or a combination of standard screening approaches like chromatography, mass spectrometry, ultraviolet detection, or fluorescence-based screening. However, this reduces the efficiency considerably as the poor-quality food has already passed the costly and tedious production process. These analytical techniques are also limited by large test sample requirements, intricate pretreatments, and the need for well-trained staff (Mishra et al. 2018). Hence, it is crucial to develop new and improved techniques and sensing devices that can detect traces of impurities within the sophisticated matrix of edible products with high sensitivity and great precision in less amount of time (Liu et al. 2018a, b).

The unprecedented advancement in nanotechnology has led to extraordinary breakthroughs in the field of food inspection, diagnostics, and environmental sensing. In recent years, nanomaterials, organic as well as inorganic, are utilized in their pristine and functionalized forms in nanosensors. Owing to their small size (less than 100 nm) and unique physicochemical characteristics, nanomaterial-based food monitoring systems are capable of effectively detecting tiny molecules of contaminants. They offer a large surface area which can be further fine-tuned by controlling the size, shape, and size distribution. To take their exclusive surface-dependent properties one notch up, surfaces of nanomaterials are decorated with various

functional groups and/or biological and chemical receptors, which enhances the affinity as well as stability of resulting nanosensors. Nanosensors exhibit outstanding biocompatibility, high sensitivity, improved selectivity, low detection limit, faster response time, thus boosting its quality and efficiency (Chandra et al. 2012; Choudhary et al. 2016; Deka et al. 2018; Mahato et al. 2018; Verma et al. 2019). A tremendous amount of research work has been focused on the synthesis and application of nanomaterials in food quality assessment. Some common nanomaterials used in sensing applications are: carbon-based nanomaterials (Gupta et al. 2019; Nehra et al. 2019; Pan et al. 2019; Yang et al. 2018), like graphene (Liu et al. 2017a, b; Parate et al. 2020; Vanegas et al. 2018; Wang et al. 2018), graphene oxide (GO) and reduced graphene oxide (rGO) (Karthik et al. 2018; Zhou et al. 2018), MXenes (Khan and Andreescu 2020; Szuplewska et al. 2020; Wu et al. 2018a, b; Xie et al. 2019; Zhou et al. 2017; Zhu et al. 2020), graphitic carbon nitride (g-C₃N₄) (Hua et al. 2018; Ramalingam et al. 2019; Tabrizi et al. 2017; Zhou et al. 2016), plasmonic metallic nanoparticles (Khateb et al. 2020; Loiseau et al. 2019a; Oh et al. 2017; Shams et al. 2019; Song et al. 2017), quantum dots (QDs) (Duan et al. 2019; Hu et al. 2017, 2021; Na et al. 2019; Nsibande and Forbes 2016; Yüce et al. 2018), and upconversion nanoparticles (UCNPs) (Annaram et al. 2019; Li et al. 2020a; Na et al. 2019; Yin et al. 2019). These materials are effectively incorporated as active constituents (detector/transducer) to build small-sized sensing devices capable of signal enhancement and detection of different toxins and microbes in the smallest of food samples.

Food contaminants are detected using a range of methodologies, such as surface-enhanced Raman scattering (SERS), electrochemical sensing, fluorescence methods, colorimetric methods, molecular imprinting technology (MIT), and the latest chromatographic approach (Liu et al. 2018a, b). Each class of nanomaterials offers unique advantages when used with the appropriate inspection technique. For instance, precious metal-based plasmonic nanoparticles (Ag, Au, Pt, and Pd) provide excellent optical properties, commendable extinction cross-section, and surface plasmon resonance (SPR) that can be modified with the chemical entities that surround them. This makes them ideal signal converters as well as candidates for SERS substrates. The grouping of metallic nanoparticles and Raman spectroscopy makes SERS a rapid, easy-to-use, and high sensitivity detection technique (Liu et al. 2018a, b).

On the other hand, low-cost and highly precise biosensors with carbon-based nanostructures are designed for real-time detection of harmful elements in edibles and beverages. Most of these sensors work on electrochemical, optical, and piezoelectric principles. Moreover, luminescent nanoparticle-based sensors have gained immense popularity due to the diversity of the sensing mechanisms that can be combined with them, such as direct fluorescence, energy transfer based on fluorescence resonance, bioluminescence resonance or chemiluminescence, photon induction, and electrochemiluminescence (Yüce and Kurt 2017).

This chapter focuses on the application of a range of carbonaceous, metallic, and fluorescent nanoparticles in the field of food quality assessment. The most recent studies, published within the past 4 years, have are included in this chapter, with a

particular emphasis on the role of nanomaterials in the development of inexpensive and sensitive sensors for food quality assessment and enhancement of their overall performance.

1.2 Carbon-based Nanoparticles and Their Applications in Food Safety Monitoring

Carbon-based nanomaterials are extensively used in diverse fields due to their attractive structural properties, surface chemistry, and electrical and optical characteristics. Based on the size, layers, and shapes, these materials exhibit metal-like conductivity and semiconducting behavior. Different synthetic routes and surface modification procedures can be followed to produce a range of carbonaceous nanomaterials (Yüce and Kurt 2017). Thus, the significance of carbon-based nanomaterials in sensing platforms cannot be overemphasized. The contribution of these materials in biosensing, bioimaging, and food safety and quality monitoring applications is quite noteworthy. Carbon-nanomaterials are used as platforms in biosensors working on electrochemical, optical, and piezoelectric principles. Mainly, in electrochemical sensors, these nanomaterials serve as adsorbents or transducers due to their geometrical benefits, rapid electron transfer capabilities, wide potential range, large surface area, inert nature, and excellent electrocatalytic abilities. Moreover, they provide support and surface for biological affinity agents, such as enzymes, proteins, antibodies, DNA, which enhances their sensitivity toward organic and inorganic targets (Nehra et al. 2019). Herein, the applications of three promising classes of carbonaceous nanomaterials in food quality assessment were detailed. A summary of the reviewed publications is presented in Table 1.1.

1.2.1 MXene Nanoparticles

MXene is a significant group of nanomaterials comprising two-dimensional transition metal carbides, nitrides, and carbonitrides. Since their discovery by Gogotsi and co-workers (Naguib et al. 2011) in 2011, MXenes have garnered considerable attention due to their 2D structure that can be easily modified, a large surface area with fantastic potential for functionalization, broad interlayer spacing, and optimum blend of physicochemical properties, such as high electrical conductivity, hydrophilic nature, biocompatibility, and chemical and thermal stability (Khan and Andreescu 2020). They are labeled as MXenes due to their general formula $M_n + 1X_n$ ($n = 1, 2, 3$), where M represents an initial transition metal (e.g., Sc, Ti, V, Cr, Zr, Nb, Mo, Hf, Ta) and X represents carbon, nitrogen, or both, and graphene-like structure. The wet chemical synthesis of MXenes involves selective etching of a parent 3D MAX phase, in which the sandwiched layer A (an element belonging to group 13 or 14) is removed, and M_2X , M_3X_2 , or M_4X_3 structures are obtained (Alhabeab et al. 2017). While hydrofluoric acid (HF) is a popular etchant to produce $Ti_3C_2T_x$ MXenes, other more sophisticated synthetic routes have been developed

Table 1.1 Carbon-based nanomaterials in food safety monitoring

Nanoparticle	Affinity agent	Target/s	Sensing principle	Limit of Detection	Real sample measurements	Ref
MXene (Graphite/TiC/Ti ₃ C ₂ /Chitosan)	Horse Radish Peroxidase (HRP) enzyme	H ₂ O ₂	Electrochemical	0.74 µmol/L	Yes, in milk and dried scallop	Bao-Kai et al. (2020)
MXene/Au-Pd	Acetylcholinesterase (AChE)	Paraoxon	Electrochemical	1.75 ng/L	Yes, in pear and cucumber	Zhao et al. (2020)
MXene-Ti ₃ C ₂ T _x	Acetylcholinesterase (AChE)	Malathion	Electrochemical	0.3 × 10 ⁻¹⁴ M	Yes, in tap water	Zhou et al. (2017)
MXene-Ti ₃ C ₂	Tyrosinase enzyme	Phenol	Electrochemical	12 nmol/L	Yes, in tap water spiked with phenol	Wu et al. (2018a, b)
MXene/AuNR	-	R6G, CV, MG, thiram, and diquat	SERS	1 × 10 ⁻¹² (for R6G and CV), 1 × 10 ⁻¹⁰ M (for MG), 1 × 10 ⁻¹⁰ M (for thiram), and 1 × 10 ⁻⁸ M (For diquat)	No	Xie et al. (2019)
MXene-Ti ₃ C/Au-Ag NSs	-	Carbendazim (CBZ)	Electrochemical and SERS	0.002 µM (electrochemical) and 0.01 µM (SERS)	Yes, in rice and tea	Zhu et al. (2020)
MXene/Au@Pt nanoflower	5'-Nucleotidase-xanthine oxidase and bovine serum albumin (BSA)	Inosine monophosphate (IMP)	Electrochemical	2.73 ng/mL	Yes, in chicken, pork, beef, and lamb	Wang et al. (2020a, b)
P-g-C ₃ N ₄ /O-MWCNT	-	Cd(II), Hg(II), Pb(II), and Zn(II)	Electrochemical	8 and 60 ng/L	Yes, in cabbage, capsicum, and noodles	Ramalingam et al. (2019)

(continued)

Table 1.1 (continued)

Nanoparticle	Affinity agent	Target/s	Sensing principle	Limit of Detection	Real sample measurements	Ref
g-C ₃ N ₄ -TiO ₂	Aptamer, 5'-NH ₂ -(CH ₂) ₆ -5' TACTA ACGGTACAAGCTACCCAG GCCGCCAACGTTGACCTA GAAAGCACTGCCAGACCCGA ACGTTGACCTAGAAAGC-3'	Tropomyosin (TROP)	Photoelectrochemical	0.23 ng/mL	Yes, in human serum	Tabrizi et al. (2017)
g-C ₃ N ₄	-	Vanillin	Electrochemical	4 nM	Yes, in milk, tea, and biscuits	Fu et al. (2020)
g-C ₃ N ₄ and C-dots/3DGH	Aptamer, 5'-GCA ATG GTA CCGG TAC TTC CCC ATG AGT GTT GTG AAA TGT TGG GAC ACT AGG TGG CAT AGA GCC GCA AAA GTG CAC GCT ACT TTG CTA A-3'-NH ₂ -(CH ₂) ₆	<i>E. coli</i>	Photoelectrochemical	0.66 CFU/mL	Yes, in diluted milk	Hua et al. (2018)
C ₃ N ₄ NTs/ Pt NPs	Molecular Imprinted Polymer (MIP)	Atrazine (ATR)	Electrochemical	1.5 × 10 ⁻¹³ M	Yes, in wastewater samples	Yola and Atar (2017)
Graphene	Antibody	Histamine	Electrochemical	30.7 μM	Yes, in fish broth	Parate et al. (2020)
Cu-plated Graphene	Diamine oxidase (DAO) enzyme	Biogenic Amines (BA)	Electrochemical	11.6 μM	Yes, in fresh and fermented fish paste	Vanegas et al. (2018)
NiFeSP@Graphene	-	Paraoxon Ethyl (PE)	Electrochemical	3.7 nmol/L	Yes, in tap water, tomato juice, and cucumber juice	Aghaie et al. (2019)
Graphene-AuNPs	CRD of hGal-3	Lactose	FET	200aM	No	Danielson et al. (2020)

Au-ZrO ₂ -Graphene Nanosheets	-	Methyl parathion (MP)	Electrochemical	1 ng/mL	Yes, in Chinese cabbage	Gao et al. (2019)
Ag@GO Nanoribbons	-	Methyl parathion (MP)	Electrochemical	0.5 nM	Yes, in fresh cabbage, green beans, strawberry, and nectarine fruit	Govindasamy et al. (2017)
GO-wrapped Fe ₃ O ₄ @Au particles	Aptamers sequence: 5'-SH-TCTAAAAATGGCCAAAGAAA CAGTGAC TCGTTGAGATACT-3' (apt 1) and 5'-TAMRA-TCTAAAAATGGCCAAAGAAA CAGTGACT CGTTGAGATACT-3' (apt 2).	<i>V. parahaemolyticus</i>	SERS	14 CFU/mL	Yes, in fresh salmon	Duan et al. (2017)
PtM/rGO	-	Methyl parathion (MP)	Electrochemical	1.8 nM	Yes, in water samples (tap and lake) and vegetables/fruit	Karthik et al. (2018)
Cu ₂ O/rGO	-	Sunset yellow (azo food colorant)	Electrochemical	6.0 × 10 ⁻⁹ mol/L	Yes, in carbonated drinks, orange juice, and candies	He et al. (2018)

over recent years. The etching is often followed by ultrasonic delamination to acquire a stack of MXene sheets that are single layered or only a few layers thick. As the last step, intercalation via huge cations is performed to increase the available surface area and improve efficiency (Szuplewska et al. 2020). Unlike other 2D nanomaterials, the intercalation capacity of MXenes is excellent.

While MXenes are attractive materials for catalytic and photocatalytic processes, energy storage, and biotechnological applications, they are particularly useful for biosensing and food quality assessment. The unsaturated, hydrophilic, and conductive surface of MXene-based platforms can be readily decorated with a range of biomolecules (proteins/enzymes) (Bao-Kai et al. 2020; Zhou et al. 2017) and nanoparticles (Zhao et al. 2020; Zhu et al. 2020) to predominantly enhance the selectivity, sensitivity, and stability of sensors and/or one-time tests using them. A recent study explored the effect of tailoring the surface of pristine Ti₃C₂-MXene with noble-metal NPs and ceramic oxide on its ecotoxicity, phytotoxicity, and antimicrobial characteristics. It was reported that surface modification could alter the toxic properties of pure MXene, making some tailored materials showing undesirable toxicity; however, the antimicrobial response against both Gram-positive and Gram-negative bacteria was positively affected (Rozmyslowska-Wojciechowska et al. 2019). Many MXene biosensors with low detection limits and fast response times have been proposed to detect toxins, microbes, pesticides, and pollutants found in food and drinks (Bao-Kai et al. 2020). To detect phenol in drinking water, Wu et al. (2018a, b) produced an ultrasensitive biosensor featuring an MXene-Ti₃C₂ platform. MXene nanosheets were obtained by etching its parent MAX, i.e., Ti₃AlC₂ in HF, which were then casted on glassy carbon electrode (GCE), and tyrosinase enzyme was immobilized on its surface. Tyr-MXene-Chi/GC biosensor exhibited outstanding bioanalytical tendency and detected phenol in real water samples without any mediator. It was also found to be highly sensitive with low response time and detection limits. In another study, Zhou et al. (2017) similarly fabricated MXene-Ti₃C₂ nanofilms and cast them onto GCE with chitosan acetylcholinesterase (AChE) enzyme for the detection of a toxic organophosphorus pesticide-malathion. Spike recovery tests in tap water proved the reliability of the proposed amperometric sensor with a low LOD and broad linear range. Another enzymatic biosensor was designed by Zhao et al. (2020) for the detection of highly toxic organophosphorus pesticides found in edible plants and agricultural produce. The disposable sensor consisted of a screen-printed electrode (SPE) covered with ultra-thin MXene nanosheets (1.5 nm thickness), which were synthesized by etching Ti₃AlC₂ in lithium fluoride (LiF) and hydrogen chloride solution (HCl) for 1 day at 35 °C, followed by sonication in water and centrifugation at 3500 rpm for 60 min each. MXene-coated SPE was immersed in a solution of HAuCl₄ and PdCl₂, which allowed Au and Pd particles of size 30–80 nm to grow on its surface within 5 s because of self-reduction. Finally, 10 μL of AChE enzyme was immobilized on the electrode surface, and the SPE/MXene/Au-Pd/GA/AChE electrode was oven-dried for 30 min. Electrochemical impedance spectroscopy (EIS) proved that the produced MXene-based nanocomposite had sufficient conductivity, increased electrocatalytic activity, and excellent transfer of electrons. Through amperometric analysis and

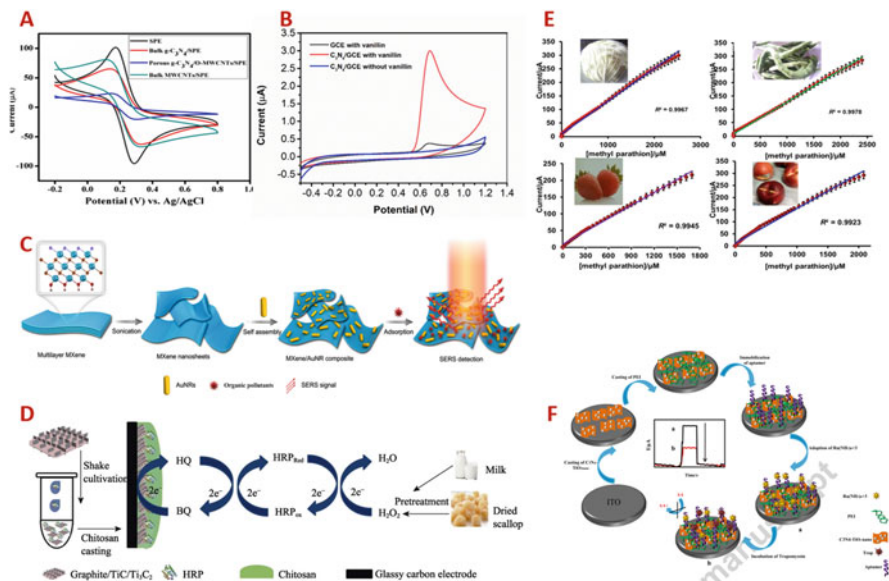


Fig. 1.1 (a) Electrochemical behavior of different modified electrodes in 5 mM $[Fe(CN)_6]^{3-4-}$ in 0.1 M KCl as supporting electrolyte at a scan rate of 50 mVs^{-1} [16]; (b) Cyclic voltammograms of bare GCE and C_3N_4 /GCE toward $10\text{ }\mu\text{M}$ vanillin in 0.1 M phosphate-buffered saline (PBS) (pH 7) [15]; (c) Schematic illustration of the fabrication of the MXene/AuNR composite and application as a substrate to SERS detection [11]; (d) Schematic illustration for the fabrication of HRP@MXene (Graphite/TiC/Ti₃C₂)/chitosan/GCE and H_2O_2 sensing principle of HRP@MXene/chitosan/GCE [6]; (e) Calibration plots for real sample analysis; [methyl parathion] (μM) vs. current (μA). (a) Cabbage, (b) green beans, (c) strawberry, and (d) nectarine fruit; (f) Schematic illustration of proposed PEC aptasensor fabrication and the sensing mechanisms employed by [17]

testing on real pears and cucumbers spiked with paraoxon, good stability and selectivity, and reliable performance of the sensor were confirmed.

Bao-Kai and co-workers (2020) synthesized an MXene-based electrochemical sensor to detect hydrogen peroxide (H_2O_2) in food (Fig. 1.1d). Firstly, 2D MXene nanosheets (graphite/TiC/Ti₃AlC₂) were prepared by mixing graphite, Ti, and Al powders with NaCl and KCl in a molar ratio 4 : 4: 1: 10 : 10. The mixture was heated and kept at $800\text{ }^\circ\text{C}$ for 5 h and then at $1100\text{ }^\circ\text{C}$ for 3 h. Subsequently, the mixture was cooled, washed, and etched with HF to obtain MXene nanosheets with a large specific surface area, high electronic conductivity, and desirable dispersion in an aqueous medium. To further enhance the electromagnetic absorption, enzyme entrapment, and electron transferability of the MXene-based platform, these sheets were arranged perpendicular to the graphite plane, forming a unique vertical junction structure. Next, GCE was uniformly coated with the fabricated MXene and Chitosan film. Finally, Horse Radish Peroxidase (HRP) enzyme was entrapped on MXene/chitosan/GCE, and no conformational alteration was observed in its secondary structure as per the FT-IR analysis. The biosensor successfully sensed the H_2O_2 traces in milk and contaminated dried scallops. The wide linear range from 5 to

1650 $\mu\text{mol/L}$, low limit of detection (LOD) of 0.74 $\mu\text{mol/L}$, high selectivity, and stability of the HRP@MXene/chitosan/GCE was attributed to the sophisticated vertical arrangement of the MXene platforms. Wang et al. (2020a, b) created a novel biosensor based on $\text{Ti}_3\text{C}_2\text{TXAu@Pt}$ nanoflowers for meat quality assessment. The enzymatic sensor effectively and rapidly detected Inosine monophosphate (IMP) in four different meat samples (chicken, beef, pork, and lamb) owing to the conductive and biocompatible MXene nanosheets decorated with bimetallic nanoflowers. GCE was polished and coated with graphene-like $\text{Ti}_3\text{C}_2\text{T}_x$ prepared by selective etching with LiF and functionalized with core-shell Au@Pt nanoflowers. Two different enzymes, namely 5'-nucleotidase-xanthine oxidase and bovine serum albumin (BSA), were immobilized on the surface of the electrode. MXene/Au@Pt platform boosted the H_2O_2 oxidation in IMP-containing meat, which resulted in electron transfer. The change in electric current was directly related to the concentration of IMP in the meat.

Following a different route, Xie et al. (2019) designed a $\text{Ti}_3\text{C}_2\text{T}_x$ -AuNRs substrate to be used in surface-enhanced Raman scattering (SERS) technique for effective sensing of problematic environmental pollutants of organic nature transferred to our food through dyes and pesticides. As shown in Fig. 1.1c, layered $\text{Ti}_3\text{C}_2\text{T}_x$ was etched with HF, and the resulting 2D MXene nanosheets were uniformly coated with Au nanorods prepared with a seedless procedure. The composite assembled on its own due to the electrostatic forces and carried abundant hot spots for SERS. The substrate detected typical organic dyes, like rhodamine 6G (R6G), crystal violet (CV), and malachite green (MG) with excellent sensitivity, reliability, and reproducibility. It even proved its efficiency as an ultrasensitive food safety sensor for more sophisticated pollutants like thiram and diquat. Furthermore, Zhu and co-researchers (2020) constructed an advanced MXene-based smart sensor with the help of machine learning techniques and proposed it to monitor harmful carbendazim (CBZ) traces in liquid and solid food items. The fabricated MXene/Au-Ag nano shuttles (NSs) can be used as electrochemical sensors as well as SERS substrate. 2D Ti_2C MXene powder was fabricated by HF etching of Ti_2AlC powder at 25 °C for 1 day, followed by centrifugation, washing, and drying. The nanohybrid was designed through ultrasonic dispersion of pristine MXene in Au-Ag NSs solution. This bifunctional platform was drop-coated on GCE for electrochemical analysis and on glass matrix for SERS analysis. Characterization revealed that the synthesized nano shuttles had a rough surface with a large area, high conductivity, commendable electrochemical behavior, and outstanding Raman enhancement. The nanosensor was highly stable and offered a broad linear range and low LOD for both electrochemical and Raman sensing. The successful tests on real samples of rice and tea showed the efficacy of these MXene-based nano shuttles in food safety and monitoring.

1.2.2 Carbon Nitride Nanoparticles

Among all the allotropes of naturally existing carbon nitride (CN), graphitic carbon nitride (g-C₃N₄) is lauded for its stability at room temperature, planar geometry, large surface area, unique physical and electrocatalytic properties, and metal-free polymeric nature (Chen and Song 2017). It features a layered, graphene-like 2D structure with sp² bonded C and N atoms arranged as a tri-s-triazine ring linked with tertiary amines. This unique structure gives it high thermal stability, chemical resistance, and a bandgap like semiconductors. It comprises nitrogen atoms and defects that act as active spots and boosts its electric conductivity (Magesa et al. 2019). Traditionally, g-C₃N₄ is fabricated in bulk via polymerization of typical precursors (like cyanamide, dicyandiamide, and melamine) by physical vapor deposition (PVD), thermal nitridation, solvothermal, chemical vapor deposition (CVD), and solid-state reaction. To obtain ultrathin single-lamellar g-C₃N₄ films, bulk material is exfoliated thermally, chemically, or ultrasonically. What makes it even more appealing for a range of applications is the resulting large surface ready to be embellished with metallic, non-metallic, and carbonaceous nanomaterials (Chen and Song 2017).

Several sensors have been designed by using g-C₃N₄ in its pristine or functionalized form for the detection of food colorants, antimicrobial remnants, metal ions, and toxic pesticides. In research by Fu et al. (2020), layered C₃N₄ nanosheets were fabricated by thermal oxidation of melamine precursor and coated as an absorbent unto the GCE. This sensor offered fast and simple monitoring of vanillin in edibles. A comparison of GCE with and without the C₃N₄ layer is shown in Fig. 1.1b in terms of vanillin's electrochemical behavior. The C₃N₄/GCE showed a decline in background current when no vanillin was present, and the oxidation signal was enhanced at a lower overpotential. This further confirms that vanillin receives an electrocatalytic response from C₃N₄. Hence, it can be deduced that C₃N₄ reportedly increased the active-specific area and electrochemical activity of the electrode. The resultant vanillin sensor had an LOD of 4 nM and a wide linear range of 20 nM–10 μM and 15 μM–200 μM, when tested on real milk, tea, and biscuits. Ramalingam and co-workers (2019) designed a highly selective sensing matrix created from porous g-C₃N₄ nanosheets and oxidized multiwalled carbon nanotubes, named p-g-C₃N₄-NSs/O-MWCNTs. Fabrication of the platform involved a single-step oxidation process in which bulk carbon nitride was mixed with bulk MWCNTs in potassium dichromate and sulfuric acid. As surfaces of both materials underwent acid functionalization, 1D O-MWCNTs was firmly embedded into the pores of 2D g-C₃N₄, and a 3D nanocomposite platform was obtained. After ATR-IR spectroscopy, XRD, and TEM analysis, the platform was drop-casted on SPE. The cyclic voltammograms of different electrodes shown in Fig. 1.1a reveal that P-g-C₃N₄/O-MWCNTs/SPE has a greater Δ*E*_p value, which can be attributed to the carboxylic acid and hydroxyl groups (carrying a negative charge) attached to the surface. Owing to the uninterrupted electron transfer and excellent electrocatalytic activity of the tailored SPE, the biosensor detected four heavy metal ions Zn(II) Pb(II), Hg(II), and Cd(II) in spiked vegetables and noodles simultaneously by using

anodic stripping voltammetry technique. The biosensor showed great accuracy, sensitivity, and selectivity.

In a pioneering study, Tabrizi and group (2017) built a photoelectrochemical aptasensor driven with visible light and made the most of the high photoactivity of $g\text{-C}_3\text{N}_4/\text{TiO}_2$, as shown in Fig. 1.1f. The produced sensor was used to detect tropomyosin (an allergen found in seafood) and showed a promising range up to 400 ng/mL and a low LOD of 0.23 ng/mL. They synthesized $g\text{-C}_3\text{N}_4$ by heating melamine at a rate of 3 °C/min up to 520 °C and kept the product at the same temperature under argon flow for 4 h. Consequently, it was dissolved with TiO_2 and deposited over the ITO electrode, followed by a coating of polyethyleneimine (PEI). Finally, the amine terminal TROP probe was attached to the electrode surface, and the cleaning procedure was followed. This PEC aptasensor was tested on diluted human serum samples and demonstrated a decreasing photocurrent intensity with a corresponding increase in the concentration of tropomyosin. Hua et al. (2018) followed the synthetic route detailed in (Tabrizi et al. 2017) to prepare $g\text{-C}_3\text{N}_4$ and modified one side of the ITO electrode with it, whereas the adjacent side was functionalized with carbon quantum dots embedded into 3D graphene hydrogel (C-dots/3DGH) to build an ultrasensitive ratiometric PEC biosensor. The aptamer was coated onto the C-dots/3DGH, while $g\text{-C}_3\text{N}_4$ acted as a reference providing stable anodic current. The difference in bias voltage helped distinguish the current from the anode and cathode, and the ratio between the two was used for *E. coli* concentration monitoring. Milk samples containing different amounts of *E. coli* confirmed recovery and stability. Yola and Atar (2017) adopted an emerging technique called molecular imprinting to produce a unique electrochemical sensor that featured a C_3N_4 NTs/Pt NPs nanocomposite. The molecularly imprinted polymer (MIP) contained active spots for the determination of atrazine (ATR)—a pesticide released in water sources from where it travels into soil and agricultural products. Nanotubes of C_3N_4 embellished with Pt NPs were produced via a single-step hydrothermal method and deposited onto a clean GCE. ATR was then imprinted onto the electrode via cyclic voltammetry (CV). The prepared electrode was then used for ATR detection in contaminated water fractions. According to the sample tests, the voltammetric sensor exhibited good recovery, low LOD, high stability and selectivity, and low response time.

1.2.3 Graphene and Derivatives

The discovery of graphene in 2004 (Novoselov et al. 2004) marked a new era in nanotechnology and opened doors for a myriad of applications, one of which is food quality monitoring and sensing. Flaunting a honeycomb-like rigid framework made up of a single layer of sp^2 -hybridized carbons, graphene has served as a stepping stone for the fabrication of 0D (nanoparticles and fullerenes), 1D (single-walled nanotubes, nanorods, and nanowires), and 3D (graphite, nanocomposites) structures. Its exceptional mechanical strength, attractive chemical and thermal properties, unparalleled electron transfer capability, and generous surface area is bound to

spike every scientist's interest (Magesa et al. 2019). Some conventional methods for graphene synthesis are chemical vapor deposition (CVD), epitaxial growth, laser ablation approach, and silicon carbide decomposition. However, a recent study by Parate et al. (2020) proposed the aerosol jet printing (AJP) technique as a low-cost method to produce a graphene-based histamine sensor that could find application in identifying contaminated seafood and prevent consequent allergic reactions. Using graphene-nitrocellulose ink, an interdigitated electrode (IDE) was printed on a polyimide substrate and modified with oxygenated moieties via annealing. Histamine antibody was then covalently embedded on graphene, and the final product was used to detect histamine in real fish broth electrochemically. The sensor showed a broad detection range with a low LOD, and the detection was completed in around half an hour in liquified food samples.

Another low-cost amperometric food safety biosensor was designed by Vanegas et al. (2018) by reagents and materials procured from local stores. The proposed sensor showcased a system of electrodes prepared with a laser scribed graphene (LSG) technique. This synthetic approach transformed the sp^3 carbon of polyimide into an sp^2 -hybridized allotrope of graphene. The electrode possessed a multilayer porous graphene structure, plated with copper nanocubes, and functionalized with diamine oxidase (DAO). The biofunctionalized, Cu-coated LSG electrodes were designed to offer selectivity and electrochemically detect high concentrations of biogenic amines (BA), such as histamine, cadaverine, tyramine, and/or putrescine, in food to prevent food poisoning and food intolerance. The tests performed on real fish samples, before and after fermentation, confirmed that the LSG-Cu-DAO biosensor could detect histamine with an LOD of 11.6 μM , and a response time of 7.3 s.

Rouhani (2019), in his computational analysis, discussed the electronic efficiency of fluorographene and its role in the detection of ammonia and typical amines (like methylamine, dimethylamine, and trimethylamine) that can help sense contaminated seafood. Since inadequate adsorption of gas molecules limits the sensing ability of pristine graphene, fluorine-doping could be an effective method to overcome this limitation. With the help of the density functional theory (DFT) model, the adsorption of ammonia and amine molecules was tested for pristine and fluorine-doped graphene sheets. The theoretical findings confirmed that gas molecules showed better adsorption on fluorinated sheets as more precise signals were received due to high electron transfer and electrical conductivity. Hence, such a sensor could be used to assess the quality of seafood and detect fish spoilage. Aghaie and co-workers (2019) followed a sophisticated fabrication route to produce an enzyme-free sensor featuring a graphene-based bimetallic (NiFe) phosphosulfate nanocomposite to boost the voltammetric signals received from paraoxon ethyl (PE: an organic pesticide found in food items) and facilitate its detection. Since the target OP has an aromatic structure, it experiences desirable π - π stacking interactions with graphene. The NiFe phosphosulfate further ensures that PE sticks to the surface of GCE. PE was adsorbed completely into the electrode within 5 min, and a tremendous increase in maximum square wave voltammetric (SWV) signals was noted, which was ascribed to the properties of the graphene-based electrode. The sensor was also tested on contaminated water and fruit and vegetable juices and was found to be

efficient. A non-enzymatic, ultrasensitive graphene field-effect transistors (G-FETs) biosensor was proposed by Danielson and his group (2020) for lactose sensing. They produced a single-layer graphene sheet enriched with uniformly distributed Au NPs and immobilized carbohydrate recognition domain (CRD) of the human galectin-3 (hGal-3) protein on its surface. Minimum voltage shifted in the negative direction during liquid gate measurement, which is characteristic for lactose, whereas a positive shift was observed for other carbohydrates. This indicates the suitability of this biosensor in detecting lactose in food.

Gao et al. (2019) used a GCE covered with graphene nanosheets decorated with gold and zirconia particles to detect methyl parathion (MP), a harmful organophosphorus pesticide. The prepared electrode provided excellent electrocatalytic activity and sensed MP with great accuracy. This was backed by the results of square wave voltammetry that showed a wide linear range of 1–100 ng/mL and 100–2400 ng/mL. For the same target pesticide, Govindasamy et al. (2017) used graphene oxide (GO) nanoribbons considering its various structural features, like tunable large surface areas, solubility in water, and high adsorption capacities for biological materials like enzymes, proteins, peptides, and nucleic acids (Chen and Nugen 2019). GO NRs were embellished with Ag NPs and loaded on an SPE, which exhibited commendable electrocatalytic activity as MP underwent reduction. Good linearity with MP concentration was observed in the calibration plots for real food items, as shown in Fig. 1.1e. In another food sensing-related assay, the authors explored the application of graphene oxide wrapped around $\text{Fe}_3\text{O}_4@Au$ particles to construct an SERS-based sensor. The aptasensor's surface carried two different aptamers separated by a magnet to serve as capture probe and SERS sensing probe, respectively. This sensor was used to detect a notorious food pathogen, *Vibrio parahaemolyticus*, by measuring the SERS intensity of TAMRA aptamer. It showed a wide linear range, i.e., between 1.4×10^2 to 1.4×10^6 CFU/mL and a low LOD of 14 CFU/mL. Tests with contaminated fish yielded impressive recoveries in the range of 98.5–105% (Duan et al. 2017).

The reduced form of graphene oxide (rGO) is also suitable for electrode fabrication (Yang et al. 2018). Karthik and co-workers (2018) designed an electrochemical sensor for MP monitoring but used reduced graphene oxide (rGO) and functionalized it with 3D praseodymium molybdate (PrM) to create a novel nanocomposite. The voltammetric findings revealed lower and higher peaks for potential and cathodic current, respectively. Also, good linearity and sensitivity deemed this rGO-based composite fit for MP detection. He et al. (2018) reduced graphene oxide electrochemically and combined it with Cu_2O to produce a nanocomposite, tagged as $\text{Cu}_2\text{O-ErGO}$. The fabricated nanocomposite was then deposited on GCE to detect a popular food colorant—sunset yellow. Owing to the use of $\text{Cu}_2\text{O-ErGO}$, the dye produced 25 times greater anodic peak. The LOD of the sensor was as low as 6.0×10^{-9} mol/L, which is even better than electrodes prepared with precious metals. Real samples were used to establish the performance of the sensor.

1.3 Metallic Nanoparticles and Their Applications in Food Safety Monitoring

Over the years, noble-metallic nanoparticles have drawn considerable attention due to their fascinating physical and chemical properties. The metallic nanoparticles can be easily synthesized and modified with various chemical and biological functional moieties such as antibodies, peptides, DNA, and drugs. Therefore, they have myriads of applications in biotechnology, drug delivery, biosensing, and imaging. Furthermore, the unique optical properties of plasmonic nanoparticles lead to the development of various imaging modalities such as MRI, PET, CT, and SERS. The optical properties of these noble-metal nanoparticles have attractive aspects under investigation. The metallic nanoparticles exhibit plasmonic properties, i.e., surface plasmon resonance (SPR) and localized surface plasmon resonance (LSPR). The SPR phenomenon occurs when a beam of light is incident on the metal nanoparticles. The free surface electrons collectively oscillate in a phase with the incident light. When the frequency of the collective oscillations is approximately the same as the incident light, or the resonance condition occurs, such a phenomenon is known as LSPR. In brief, plasmonic properties deal with the interaction of light with metallic nanostructures to enable optical measurements that are related to the binding events. These help in deriving precious information about the character of the molecules (Kahraman et al. 2017; Liu et al. 2020a, b). SPR and LSPR property generally are governed by several factors such as the size, shape, geometry of the nanoparticles. Further, dielectric properties of the surrounding medium and the interparticle-coupling interactions play an essential role in the SPR and LSPR properties of nanoparticles (Yang et al. 2016).

Over the past decades, plasmonic nanoparticle-based detection sensors have gained considerable attention due to their tuned absorption wavelength, electromagnetic control, and single-molecule detection capability. Plasmonic sensors belong to a class of optical affinity biosensors. When the recognition element captures the target analytes, it provides a measurable signal (Kurt et al. 2019). The commonly used plasmonic nanoparticles are gold (AuNPs) and silver colloidal nanoparticles (AgNPs) employed to immobilization several recognition elements (antibodies, aptamers, and peptides). Due to the unique optical and physical properties, plasmonic sensors are indispensable for real-time and label-free analyte detection from various complex matrices. These can also be employed for the ultrasensitive detection of targeted substances from clinical samples and food matrices (Zhan et al. 2020). The biosensing schematic based on the plasmonic nanomaterials and various detection methods are presented in Fig. 1.2a.

1.3.1 Gold Nanoparticles (AuNPs)

Gold nanoparticles (AuNPs) are the most used plasmonic nanomaterials owing to their well-characterized LSPR phenomenon. The LSPR of AuNPs yields a high absorption coefficient and scattering properties within the visible wavelength to the

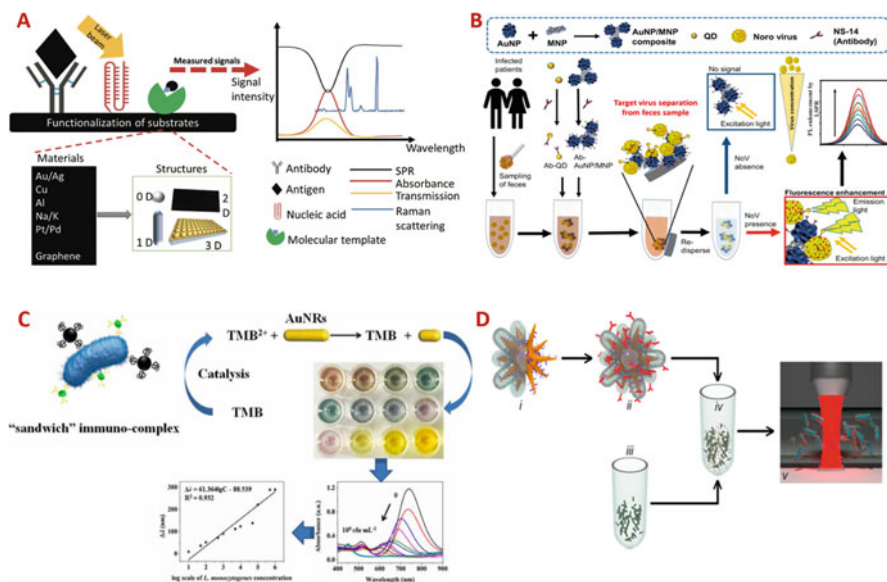


Fig. 1.2 (a) The schematic of the biosensing system by using plasmonic nanomaterial. (b) The human norovirus detection using LSPR-amplified magneto-fluoroimmunoassay. (c) A multi-colorimetric assay based on the plasmonic properties of AuNRs for the detection of *L. monocytogenes*. (d) Schematics of the SERS-based *L. monocytogenes* detection. (i) Fabrication of SERS-encoded GNSs (ii) Conjugation of the mAb C11E9 (iii) Sample bacteria at specific concentration (iv) incubation with SERS tag for recognition (v) SERS detection in a microfluidic channel. Figures A, B, C, and D are adapted from the references (Liu et al. 2019, 2020a, b; Rodríguez-Lorenzo et al. 2019; Takemura et al. 2019), respectively

near-infrared range (Caucheteur et al. 2015). The spectral characteristics of LSPR produced by AuNPs are independent of size, shape, and the local dielectric environment. Therefore, after binding the target analyte, the refractive index shift could be used to monitor the molecular binding events. Several studies on the implication of LSPR of AuNPs for detecting pathogens or toxins associated with food safety have been demonstrated.

Oh et al. (2017) developed a label-free portable LSPR platform for the selective detection of *Salmonella typhimurium* from the pork meat sample (Oh et al. 2017). The *S. typhimurium* is considered as the "zero tolerance" microorganism in food samples and is the cause of acute gastroenteritis in humans. The sensor involved the self-assembly of AuNPs (20 nm) on a glass substrate of 5 cm × 0.8 cm (length × width). The aptamers were used as a recognition probe to capture the target bacteria. The sensor exhibited an LOD of around 10^4 CFU/mL in half an hour. Further, the developed sensor detected *S. typhimurium* from the spiked pork meat sample with an LOD of 1.0×10^4 CFU/mL without any pre-enrichment steps. The study also showed that the AuNPs immobilized plasmonic chip did not affect the food matrix or background contaminant of microflora. In another study, Yaghubi et al. 2020, developed a high-resolution optical method by employing the LSPR

property of spherical AuNPs for the detection of *E. coli* O157:H7 (Yaghubi et al. 2020). The *E. coli* O157:H7 is one of the most important foodborne pathogens, which causes developing hemorrhagic colitis and hemolytic uremic syndrome. The sensor was developed by conjugating the specific anti-*E. coli* O157:H7 chicken antibody (IgY) under the specific pH of the nanoparticles. The characterization was performed by several analytical methods such as UC-VIS and DLS. The sensitivity was found to be 10 CFU/mL, i.e., the LSPR of AuNPs (λ max) redshifted from 530 nm to 543 nm in the presence of 10 bacteria. *E. coli* O157:H7 was also detected in complex food matrices within 2 h.

Apart from detecting bacteria from the food matrices, plasmonic sensors have also been adopted to detect foodborne viruses. Norovirus is a foodborne virus that causes gastroenteritis, non-bloody diarrhea, vomiting, stomach pain, and a significant public health concern worldwide. Su Heo et al. 2019, developed a peptide-guided plasmonic biosensor to detect the human norovirus as well as the capsid proteins (Heo et al. 2019). The LSPR chip was prepared by using colloidal AuNPs on a glass substrate treated with APTES. During this process, AuNPs (16–18 nm) were immobilized on the APTES-treated glass substrate (≈ 50 particles/ 200×200 nm), and the peptide (recognition probe) was immobilized using cysteine-gold conjugation chemistry. The performance of the sensor was examined by LSPR signals, and the analyte-specific binding event was proportional to the absorbance of the LSPR signal. The LOD was found to be 0.1 ng/mL for noroviral capsid protein and around 10 copies/mL for the norovirus. The plasmonic sensor was able to detect the norovirus capsid protein from complex tissue culture media such as MEM and FBS. Takemura et al. (2019), developed another LSPR-amplified magneto-fluoroimmunoassay platform to detect the norovirus from the complex media (Takemura et al. 2019). They synthesized AuNPs with magnetic nanoparticles composite, and the anti-norovirus antibody was conjugated with CdSe quantum dots (QDs). This nanohybrid composite performed by the enhanced magnetic field and the high LSPR effects of AuNPs, which separates the norovirus from the matrices. The target norovirus-like particles were found in a linear range between 1 pg and 5 ng/mL with an LOD of 0.48 pg/mL in faces. The LOD was found to be 84 copies of RNA/mL from the clinical samples without any interference from the matrices. The detailed schematic of the plasmonic biosensor for norovirus was presented in Fig. 1.2b.

Raman spectroscopy is a sensitive characterization technique constructed on the inelastic scattering of photons from the targeting molecules. It provides essential information about chemical bond formation. However, the weak signal intensity is the major drawback of its application in biotechnology. The LSPR phenomenon of AuNPs has been utilized to enhance the light scattering signal and Raman spectroscopy. The metallic nanoparticles enhance the Raman scattering of molecules immobilized at their surface, constituting the surface-enhanced Raman spectroscopy (SERS). Here, it is important to mention that the SERS phenomenon is entirely different from the SPR, which occurs at the plane surface (Loiseau et al. 2019a). Several studies have recently reported the SERS-based biosensors utilizing AuNPs by detecting specific signals from the target analytes. Duan et al. (2020), developed

an SERS aptasensor to detect multiple foodborne pathogens by SERS tags from complex food matrices (Duan et al. 2020). The sensor consists of polydimethylsiloxane (PDMS) coated with AuNPs acting as a substrate for Raman scattering. The Au-PDMS chip was chemically modified with target-specific aptamer oligonucleotides and Raman reporter, i.e., 4-mercaptobenzoic acid (4-MBA)/nile blue A (NBA) as a recognition probe to capture the target pathogens and as pathogen-specific SERS probe, respectively. The sensor facilitated sandwich assay formation by capturing the target pathogen and then binding with the SERS probe. The sensor was validated with two foodborne pathogens, *Vibrio parahaemolyticus* and *S. typhimurium*, which demonstrated an LOD of 18 CFU/mL and 27 CFU/mL, respectively.

The point-of-care detection of the foodborne pathogens was also carried out by using lateral flow immunochromatographic assays (LFIA), which is fast, easy to operate, and cost-effective. However, the low sensitivity of the assay in the presence of various matrices hinders its further applications. The limitations of the LFA are addressed by employing the LSPR properties of the AuNPs. Wu et al. (2019), developed an LFIA to detect *L. monocytogenes* and *S. typhimurium* membrane based on the principles of SERS (Wu 2019). The monoclonal antibodies for *L. monocytogenes* and *S. typhimurium* were used as the recognition probe and DTNB as the SERS tag. The SERS-based LFIA exhibited good linear response in the range of 10^2 – 10^7 CFU/mL. The LOD was found to be 75 CFU/mL for the foodborne bacteria from the milk sample.

Accumulated evidence shows the extensive use of spherical AuNPs in the plasmonic biosensor; however, recently, gold nanorods (AuNRs) have gained interest for this purpose. The LSPR of AuNRs has two absorption bands; the first one is located at 520 nm due to the transverse localized surface plasmon resonance (t-LSPR). The second one is at a higher wavelength due to the longitudinal localized surface plasmon resonance (l-LSPR) (Chen et al. 2013). The position of the LSPR can be altered by modulating the aspect ratio of AuNRs rather than their length. Hence, AuNRs have become the ideal candidates for a wide range of biomedical applications. Shams et al. 2019, developed an AuNRs-based plasmonic detection method to detect *Campylobacter jejuni* and *Campylobacter coli*, the two most critical foodborne pathogens (Shams et al. 2019). The AuNRs were modified by the specific ssDNA probes of the *cadF* gene of *Campylobacter*. The assay's sensitivity was validated by comparing the results with conventional culture methods, PCR, and RT-PCR. The sensitivity of the assay was found to be 88%, and the specificity was 100%. The LOD was found to be 10^2 copy number/mL, which is equivalent to the RT-PCR-based detection. Liu et al. 2019, developed a multi-calorimetric assay to detect *L. monocytogenes*-based on the etching of AuNRs (Liu et al. 2019). The assay is based on the TMB²⁺ etching of AuNRs, and the aptamer-modified magnetic nanoparticles were employed to concentrate on the target organism. Furthermore, to oxidize the TMB to TMB²⁺, IgY-BSA-MnO₂ NPs were chosen as an oxidase-like nano-artificial enzyme. The longitudinal shift of LSPR of AuNRs was linearly correlated with the concentrations of

L. monocytogenes ($10\text{--}10^6$ CFU/mL) under the optimal condition with an LOD of 10 CFU/mL. The schematics of the detection platform is illustrated in Fig. 1.2c.

Liu et al. (2020a, b), reported a detection platform based on AuNRs and SERS tags conjugated with target-specific aptamer molecules and Raman reporters for food pathogen sensing (Li et al. 2020a, b, c, d). The aptamers were used as a recognition probe and induced the AuNRs into different geometrical shapes, which enhanced the Raman signal of the sensing platform. The AuNRs-based plasmonic sensor detected *E. coli* O157:H7 and *S. typhimurium* with a concentration of $10^1\text{--}10^6$ CFU/mL, with an LOD of 8 CFU/mL from spiked food samples. Loiseau et al. (2019a, b), developed a homogenous plasmonic sensor for staphylococcal enterotoxin A (SEA) sensing by the naked eye (Loiseau et al. 2019b). SEA causes food poisoning and toxic shock syndrome (TSS) produced by *S. aureus*. The principle lies in the metallic nanoparticles' LSPR properties, where the small redshift ($\sim 2\text{--}3$ nm) could be observed and visually detectable after binding of the target. Two types of nanoparticle systems were synthesized, i.e., Au inside Ag nano-shells (Au@AgNPs) and Ag inside Au nano-shells (Ag@AuNPs). The nanoparticles' thickness and surface chemistry were controlled by anti-SEA antibody, and the LSPR band was tuned near 495 (Ag@AuNPs) and 520 nm (Au@AgNPs), respectively. After the target's binding, SEA, a large redshift of the LSPR band, was observed, and visual detection was enabled. The LODs were found to be 0.2 and 0.4 nM for Au@AgNPs and Ag@AuNPs, respectively. The visual color changed from orange to red, which was visible by the naked eye. Thus, the plasmonic sensor showed potential for medical diagnostics and environmental screening.

Apart from AuNPs and AuNRs, gold nanostars are (GNSs) also used as a plasmonic nanomaterial for the development of biosensor. Rodríguez-Lorenzo et al. (2019), demonstrated the use of GNSs paired to the antibody to detect *L. monocytogenes* from the food samples (Rodríguez-Lorenzo et al. 2019). The detection was achieved in a microfluidic cartridge under a flow in real-time. The assay was also able to distinguish from *L. monocytogenes* and *Listeria innocua* in 100 s. The schematic of the GNSs-based sensor was represented in Fig. 1.2d. Khateb et al. (2020), also described a label-free aptasensor for *Staphylococcus aureus* detection (Khateb et al. 2020). The plasmonic sensor exploited gold nano-disks' LSPR properties, and the aptamer was used as a recognition element. The gold nano-disks were fabricated on a glass substrate. The sensing device was used to detect *S. aureus* from pure culture and artificially contaminated milk samples with an LOD of 10^3 CFU/mL. Furthermore, the sensor required no pre-concentration steps, and the total turn-around time of detection was 30 min. From the above sections, it could be concluded that the application of gold nanoparticles, gold nanorods, and gold nanostars could be used in plasmonic biosensors for the food safety assessment. Apart from antibodies and aptamers, sugar receptors (Kaushal et al. 2019) can also be utilized for foodborne pathogen detection. The quantification of the sensor can also be achieved by different methods such as spectroscopic method, dark field microscope, and micro-spectroscopy system.

1.3.2 Silver Nanoparticles (AgNPs)

Recently, an investigation on anisotropic morphologies of metallic NPs have been carried under large scale due to the structural, optical, electronic properties and are superior to spherical NPs. Notably, the most striking feature of anisotropic lies “in the appearance of plasmon band at a longer wavelength (near-infrared region) than that of spherical NPs” (Loiseau et al. 2019a). Inspired by the AuNRs, silver nanorods (AgNRs) were synthesized by using ascorbic acid to reduce the silver nitrate (AgNO_3) with NaBH_4 and cetyltrimethylammonium bromide (CTAB). Researchers also demonstrated the synthesis of flower-like AgNPs used as SERS substrate. Another interesting morphology of Ag is silver nanoplates (AgNPLs), where the lateral dimensions are more extensive than their heights. These anisotropic silver nanoplates have vastly been used in SERS, photovoltaics, and plasmonic biosensing. Like the AuNPs, AgNPs also demonstrate unique LSPR properties and utilize it for the biosensing application. Colloidal AgNPs are yellow and display an absorption band around 380 nm in the visible range of the electromagnetic spectrum (Lee and Jun 2019). This facilitates the colorimetric detection of the target analytes by inducing the LSPR band changes.

The application of the plasmonic nature of the AgNPs was used in a surface plasmon resonance based on a fiber-optic (FOSPR) sensor for the detection of *E. coli* O157:H7 in water and juice (Zhou et al. 2018). The antimicrobial peptide, i.e., Magainin I, was used as a recognition element to capture the target pathogen. The signal was amplified by AgNPs-reduced graphene oxide nanocomposites (AgNPs-rGO) covered with a gold film. The SPR resonance wavelength presented a linear relationship with the target bacteria at a concentration from 1.0×10^3 to 5.0×10^7 CFU/mL with an LOD of 5.0×10^2 CFU/mL, under the optimized experimental conditions. The FOSPR displayed 1.5 times higher sensitivity as compared to the sensor fabricated with only AgNPs. Furthermore, the sensor was directed to the real-time sensing of *E. coli* O157:H7 in food samples such as water, fruit, and vegetable juice. Zhao et al. (2016), developed a colorimetric method based on the LSPR of silver nano prisms (Zhao et al. 2016). In the presence of enzyme catalase, the redox balance of silver nano prism disrupted, leading to the change in the particles' size and a color shift from blue to purple, red, orange, and yellow. The color transition of Ag colloidal solutions provided a quantification of *E. coli* (10^6 – 10^7 CFU/mL). The ability of this method to detect *E. Coli* was also confirmed from the contaminated lettuce leaf. Hassan et al. (2021), developed a SERS-based detection method using the flower-like silver nanoparticles to detect pesticides (methomyl, acetamiprid-(A.C.) and 2,4-dichlorophenoxyacetic acid-(2,4-D) residue) residue from the foodstuff (Hassan et al. 2021). The results exhibited a linear relation between the SERS signal and the pesticide concentration. The LOD of the sensor was found to be 5.58×10^{-4} , 1.88×10^{-4} , and 4.72×10^{-3} $\mu\text{g/mL}$. Table 1.2 represents various plasmonic nanoparticles, their target analytes, and the LOD of each developed sensor. From the preceding sections, it can be concluded that the applications of plasmonic nanoparticles for biosensing are enormous. Current challenges include accurate control of the size, shape, and functionalization of

Table 1.2 Different plasmonic nanoparticles, sensing principle, and limit of detection

Nanoparticle	Affinity agent	Target	Sensing Principle	LOD (CFU/mL)	Real sample measurement	Ref.
AuNPs	Antibody	<i>Campylobacter jejuni</i>	SPR	4×10^4	NA	Masdor et al. (2017)
AuNPs	Antibody	<i>E. coli</i> O157:H7	Plasmonic lateral flow assay	100–600	Liquid food system	Ren et al. (2019)
AuNPs	Antibody	<i>E. coli</i> O157:H7	Colorimetric	50	Chicken food sample	Zheng et al. (2019)
Au nano bones	Aptamer	<i>E. coli</i> O157:H7	SERS	3	NA	Zhou et al. (2020a, b)
AuNPs with starch magnetic beads (AuNP@SMBs)	Antibody	<i>E. coli</i> O157:H7	SERS	10	NA	You et al. (2020)
AuNRs@SiO ₂	Antibody	<i>E. coli</i> O157:H7	SERS	10	NA	Song et al. (2017)
Flower-shaped AuNPs	ssDNA	<i>Listeria monocytogenes</i>	Colorimetric	48–4 ng (<i>hly</i> A gene) 100.4 (genomic DNA)	NA	Du et al. (2018)
AuNRs	Antibody	<i>Staphylococcus aureus</i>	Colorimetric detection	476	Chinese cabbage and beef samples	Pang et al. (2019)
AuNRs	Peptide	<i>E. coli</i> <i>S. aureus</i>	LSPR	46 (<i>E. coli</i>) and 89 (<i>S. aureus</i>)	NA	Chen et al. (2018)
AuNR@Pt	Antibody	<i>Campylobacter jejuni</i>	SERS	50	Milk sample	He et al. (2019)
AuNRs	Antibody	Aflatoxin B1	Plasmonic ELISA	22.3 pg/mL	NA	Xiong et al. (2018)
AuNPs	Single-stranded oligonucleotide	<i>Salmonella</i> spp.	Colorimetric	10	Blue berried and chicken meat	Quintela et al. (2019)

(continued)

Table 1.2 (continued)

Nanoparticle	Affinity agent	Target	Sensing Principle	LOD (CFU/mL)	Real sample measurement	Ref.
AuNRs	Antibody	<i>E. coli</i>	SERS	10	NA	Bozkurt et al. (2018)
Plasmonic nanorod array	Antibody	<i>S. aureus</i>	SERS	17.8	NA	Zhang et al. (2018)
AgNPs	Antibody	<i>E. coli</i> O157:H7, <i>Staphylococcus aureus</i> , and <i>Salmonella</i>	SERS	NA	NA	Wei et al. (2018)
Au nanoflower	Antibody	<i>E. coli</i> O157:H7	Scattering	2.7	Pasteurized milk	Zhan et al. (2019)
Au nanodimers	Aptamer	<i>S. typhimurium</i>	Raman Spectroscopy	35	NA	Xu et al. (2018)
Spiny AuNPs	Aptamer	<i>S. typhimurium</i>	SERS	4	Pork sample	Ma et al. (2018)
Fe ₃ O ₄ @Au	Antibody	<i>Vibrio parahaemolyticus</i>	SERS	14	Salmon sample	Duan et al. (2017)
AuNPs	Antibody	<i>Salmonella</i>	SPR	7.6 × 10 ⁶	Chicken meat	Wang and Park (2020)

NPs. However, the large-scale and low-cost synthesis with uniform size and shape will promote plasmonic nanoparticles for its wider application.

1.4 Fluorescent Nanoparticles and Their Applications in Food Safety Monitoring

The working principle of the methods that depends on fluorescent systems is the emission of fluorescent nanomaterial signals after exposure to radiation with a predefined level of energy, called excitation wavelength. In other words, absorption and emission of fluorescence radiation are considered critical factors in these fluorescence-based techniques. Various fluorescent nanomaterials, including quantum dots, upconverting nanoparticles, graphene, and carbon quantum dots, have been utilized to detect toxins, allergens, and other food-related pathogens. This section describes such nanoparticles (NPs), their general structural and optical features, and their applications in food safety assessment (Pehlivan et al. 2019).

1.4.1 Quantum dots (QDs)

As a semiconductor crystalline nanostructure, QDs consist of components that belong to groups II–VI or III–V of the periodic table (Matea et al. 2017). Their color is influenced by the particle size, which is smaller than 10 nm, benefiting from quantum confinement. Considering this phenomenon, along with other tunable features, they have been more frequently used in sensing assays in comparison with other NPs (Nsibande and Forbes 2016). Structurally, these inorganic fluorophores are made up of a core element and covering shell. Regarding the core part, it is frequently composed of heavy metals, such as cadmium telluride (CdTe) as well as cadmium selenide (CdSe). Due to the higher quantum yield (the ratio of emitted photons divided by photons absorbed) of CdSe, it has been more commonly used in QDs synthesis. In stark contrast, however, the toxicity of this element and its damaging impact on nature cannot be neglected. Hopefully, scientists found that passivating the core with an inorganic shell such as zinc sulfide (ZnS) has a significant effect on increasing quantum efficiency and decreasing toxicity by blocking cadmium leakage (Bonilla et al. 2016). Besides being bandgap-tunable, and their light emission can be easily adjusted along the part of the electromagnetic spectrum ranging from 400 to 4000 nm by tuning the particle size. Reducing the particle size leads to the emission of energy at higher levels, followed by an increase in the energy gap (Wagner et al. 2019). It should be noted that the chemical composition of the core part has an impact on the emission wavelength of synthesized quantum dots. Following this, they benefit from a broader spectrum in excitation and a narrower spectrum of emission while being compared with other conventional fluorophores. The narrow emission spectrum paves the way for multiple sensing assays. Moreover, they can quench the light more effectively at a specific wavelength, which makes these NPs effective probe even under a low level of light

exposure. Furthermore, these fluorophore nanostructures have high robustness against degradation from the chemical aspect. QDs demonstrate a high spectral shift, namely Stokes shift, which is of great importance. This feature paves the way for developing fluorescence-based sensing methods using signals that are not high (Reshma and Mohanan 2019). These outstanding features of QDs make these nanostructures the best candidates for biological applications such as in vitro and in vivo imaging (Chen et al. 2008), drug delivery (Al-Nahain et al. 2013), gene therapy (Mansoori et al. 2014), and food science, including sensing of foodborne pathogens and toxins (Bonilla et al. 2016).

As an example, zoonoses, which can spread widely among human being all over the world, have become one of the main health issues over the past few years. These pathogens lead to agricultural losses and endanger the existence of billions of humans (McElwain and Thumbi 2017). Some of these zoonoses with high infection risk are *Escherichia coli* (*E. coli*), *Listeria monocytogenes* (*L. monocytogenes*), and *Brucella melitensis* (*B. melitensis*) with numerous diseases. As a result, the fabrication of biosensors for the detection of these pathogens is important in food safety. Liu et al. (2020a, b, c, d) provided peptide modified magnetic beads (MBs) by binding biotin-modified peptide to streptavidin MBs through avidin-biotin interaction, a labeling technique, and enriched the pathogens in half an hour. Following this, polyclonal antibodies were coupled with various QDs to provide detection probes. Combining peptide-functionalized MBs with multicolor QDs, fluorescence-based multiple detections of bacteria was developed successfully.

Another primary concern in food safety and ecological contamination is the remaining pesticides in food after being disposed to the water and soil. Thus, developing a sensitive and consistent technique for the detection of these residues is of great significance. For instance, adding diazinon, a liquid pesticide in agriculture, to the soil is frequently detected in the food crops, which is a severe concern for human health (Sullivan and Goh 2000). Arvand et al. (2019) provided a fluorescence resonance energy transfer (FRET)-based sensor with high selectivity for sensing this pesticide, utilizing QDs and graphene oxide (GO) as donor and quencher, respectively. They modified L-cysteine-functionalized QDs with aptamer with a high affinity for diazinon. The fluorescence emission of this conjugation was quenched by adding GO. After adding target to the system, the growth in the donor's fluorescence intensity was noticed due to the separation of aptamer from acceptor and binding to diazinon pesticide, which is a target in this sensing system (Fig. 1.3a). In this developed aptasensor, the limit of detection (LOD) achieved by their group was 0.13 nM.

Acetamiprid is an insecticide widely utilized as an alternative to other conventional ones (Jin et al. 2016). Although this compound is organic, several health risks can be provided by this insecticide for humans, causing severe contamination in the environment. Therefore, the accurate tracking of this component is vital. For this aim, an aptasensor working based on fluorescence was designed by Guo et al. (2016). In this assay, QDs and the inner filter effect of gold nanoparticles (AuNPs) fluorescent probes and quenchers. It should be noted that they used aptamers with binding affinity for acetamiprid, which can attach to the AuNPs with a negative

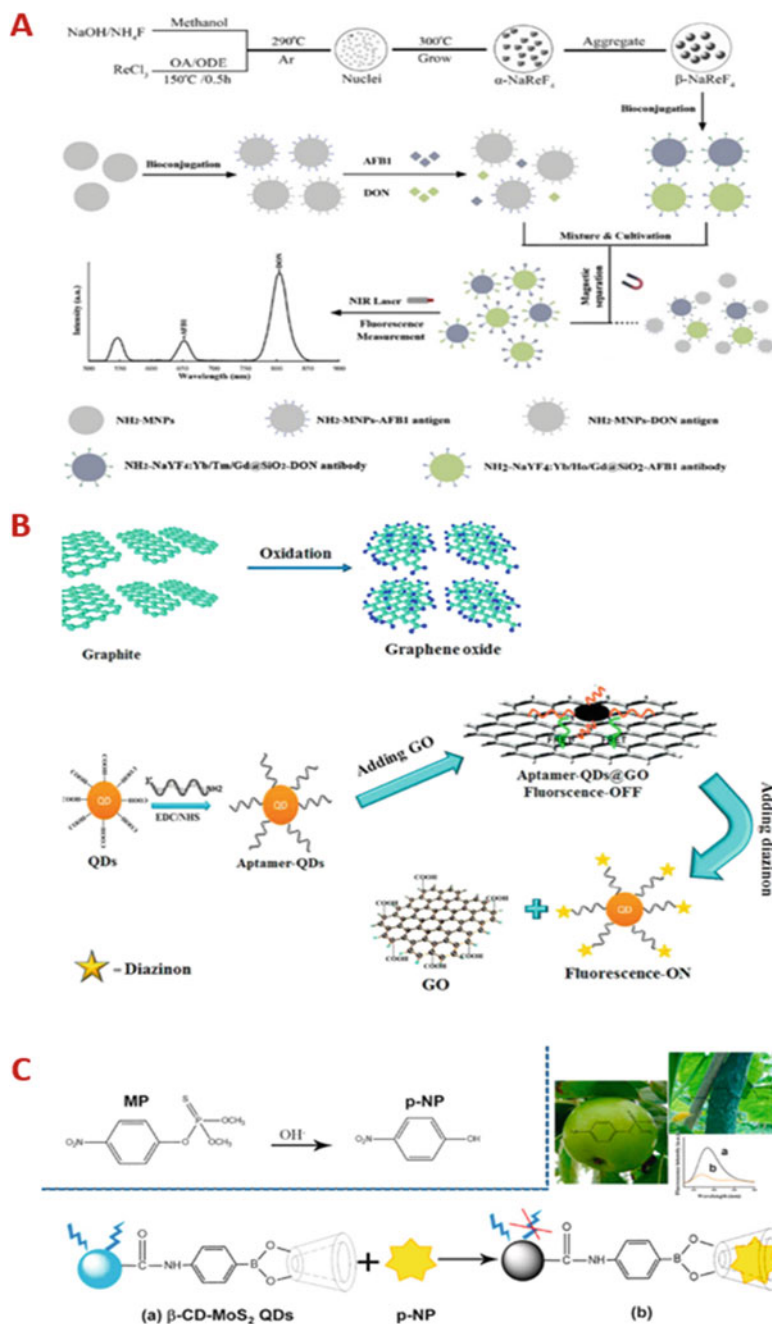


Fig. 1.3 (a) Schematic demonstration of the developing aptamer-based sensing platform for diazinon detection (Chen et al. 2016a, b), (b) Graphical illustration of UCNPs-based immunosensor designed for the detection of mycotoxins (Arvand and Mirroshandel 2019), (c) Graphical representation of MP hydrolysis along with fluorescent-based detection of MP using β -CD-MoS₂ QDs conjugation (Yi et al. 2021)

charge to protect the NPs from salt agglomeration. Thus, the inner filter effect of AuNPs contributed to the effectual quenching of fluorescence emitted by QDs. In another study, Lin et al. (2016) proposed another turn-on aptamer-based biosensor for acetamiprid. They made use of aptamer functionalized QDs along with multiwalled carbon nanotubes (MWCNTs). Before introducing the target to the system, the emission of QDs was quenched by MWCNTs. However, after the addition of the target chemical, acetamiprid, aptamer bound to it. Therefore, MWCNTs were released, which increased the intensity of fluorescence related to the QDs. Aflatoxin B1 (AFB1) is a type of mycotoxin synthesized by *Aspergillus*. As this compound can be found in food products, it poses a threat to human health due to its toxicity and cancer-causing properties. Thus, Guo et al. (2019) provided a fluorescence-based sensor to detect this mycotoxin. In this assay, a fluorescence probe was formed by coating QDs with molecularly imprinted polymers. Noteworthy is that the developed signal-on immunoassay is an effective technique for AFB1 detection in real samples.

1.4.2 Upconversion nanoparticles (UCNPs)

Upconversion is a phenomenon that can be defined as the transition of a photon from low energy levels to the ones with higher energy. Since many years ago, this process has been widely investigated in various optical designs. Along with considerable growth in nanoscience, lanthanide-doped UCNPs with enhanced efficiency and features have been provided over the last few years (Chen and Zhao 2012). This type of fluorescence NPs can emit light at a wavelength shorter than that of excitation, thanks to the anti-Stokes shift. They can convert light absorbed in the near-infrared region to ultraviolet by adjusting doping concentration and its ratio with the host component (Pehlivan et al. 2019).

In the excitation region, dopant ions with considerably high concentrations were utilized in the NIR region to prevent the autofluorescence phenomenon of biological structures in the region from ultraviolet to visible. Equally significantly, though, their emission spectrum can be improved in terms of the signal to noise ratio by reducing the fluorescence from nearby entities (Yüce and Kurt 2017). Although UCNPs exist in fewer colors than QDs, they benefit from separate and changeable excitation and emission peaks. UCNPs consist of particles at nanoscale and lattice structure; a sensitizer and an activator are the main components of these fluorescence NPs. The most common lattice is NaYF₄, which acts as a host material. The second component is a sensitizer, which significantly affects light absorption by UCNPs (e.g., Yb³⁺). Activator is the last compound of these fluorescent NPs, which has a prominent role in the emission of light at various wavelengths, leading to different colors (e.g., Er³⁺, Tm³⁺, and Ho³⁺) (Sharma and Raghavaram 2018; Wilhelm 2017). They are also desirable candidates for various applications, including bioimaging (Wen et al. 2018), solar cells (Haase and Schäfer 2011), display equipment (Park et al. 2017), biosensing, and food safety (Annavaram et al. 2019). Even though UCNPs possess remarkable capabilities for various applications, several limitations

are required to be tackled (Wilhelm 2017). For example, sulfonamides (SAs) as a type of synthetic drug are effective in the treatment of most of the animal-related microbial diseases (Shen et al. 2016). As the residues of this medicine that cause a severe risk to human health can be noticed in animal-derived foods, Hu et al. [27] developed a new method for detecting this drug. Their provided system was a FRET-based sensor utilizing erbium-doped UCNPs and colloidal AuNPs as donor and quencher, respectively. It should be noted that achieving results from low fluorescence signals, being highly sensitive and selective, and low priced are salient advantages of this turn-on sensing technique.

Molds are forming many types of mycotoxins as secondary metabolites through food settlement. Like some of the insecticides, they can cause severe harmful impacts on public health due to their cancer-causing features on the kidney and other parts of the body (Chauhan et al. 2016). AFB1 and deoxynivalenol (DON) are salient examples of which their detection is of great significance. Chen et al. (2016a, b) developed a UCNPs-based aptasensor for multiple detections of mycotoxins. In this fluorescence-based assay, they functionalized magnetic nanoparticles (MNPs). They enhanced UCNPs (NaYF_4 : Yb/Ho/Gd and NaYF_4 : Yb/Tm/Gd) with antigen and antibody to develop capture probe and signal probe. Introducing their target mycotoxins to the mixture containing the probes mentioned above led to the formation of UCNPs-antibody-antigen MNPs, and UCNPs-antibody-targets based on antibody affinity for each target. Following this, a magnetic field was applied for separating the part, which includes MNPs, and fluorescence measurements were performed for the residue part (Fig. 1.3c).

In another food safety-related assay, a biosensor working based on fluorescence was provided by Zhang et al. (2020a, b) for dual sensing of histamine and tyramine, two types of biological amines. Considering the diseases such as heart rhythm disorders and high blood pressure caused by immoderate consumption of these amines in foods, developing a useful technique for their detection is significant for human health (Erdogan et al. 2018). They functionalized NaYF_4 : Yb, Tm, and NaYF_4 : Yb, Er with antibodies with an affinity for tyramine and histamine. Moreover, magnetic microspheres were examined as binding couples of target antigens to develop a biosensing probe. The tendency of this probe for binding to a signal probe takes it into the competition with targets. Finally, the amount of tyramine and histamine was measured by fluorescence intensity obtained at 483 and 550 nm wavelengths. The LOD obtained by this biosensor for tyramine and histamine was 0.1 mg L^{-1} and 0.01 mg L^{-1} , respectively. In the case of evaluation of the provided fluorescence-based sensor specificity, nonspecific targets including phenylethylamine, serotonin, histidine, octopamine, spermidine, tryptamine, spermine, and tyrosine were tested. There was no effective interaction between antibody and other nonspecific analytes which indicates high specificity of provided sensor.

Atrazine is a type of herbicide useful for preventing undesirable vegetation. Due to its resistance in nature, it can be noticed in soil and water. This compound in food crops considering its high toxicity is cause for concern regarding human health. In one recent research, Sheng et al. (2019) modified Er-doped UCNPs with a specific antibody of atrazine to form a signal probe. In the case of the biosensing probe,

antigen-modified polystyrene magnetic microspheres were utilized. There is a competition between antigen located on biosensing probe and atrazine for being attached to the antibody to develop the immune conjugate. This step was followed by applying a magnetic field to separate conjugates and measuring fluorescence intensity. Noteworthy is that the LOD for atrazine was 2 ng L^{-1} in water samples taken from the river.

1.4.3 Other Fluorescent Nanoparticles

It has been a decade passed from the first synthesis of carbon QDs which was initially nominated as carbon NPs. However, these days they are entitled as carbon dots (CDs) due to resemblances in their physicochemical and optical features with QDs (Jelinek, 2017). Possessing a broad absorption spectrum and being chemically stable are striking features related to CDs as fluorescent NP of carbon with size between 1 and 10 nm, which have made the center of attention in recent years (Li et al. 2019). Same as other fluorescent NPs, emitting light at different wavelengths bring them to the center of attention for a variety of applications, including biosensing, drug delivery, cancer therapy, and food safety. The feature that makes these NPs stand out among others is being made up of carbons that are not toxic, and plenty of them can be found in nature. As a result, they are great candidates for application in which toxicity matters. Following this, being biodegradable due to its components is another important factor that makes these NPs an ideal alternative to other fluorescent NPs (Jelinek 2017).

Furthermore, carbons are mostly bound to other carbon atoms through sp^2 and sp^3 hybridization. They frequently have the shape of a crystal or do not have any distinct structure. It should be pointed out that the solubility of CDs in frequently used solvents can be improved by their surface modification with functional groups such as carboxyl (Molaei 2019). In food safety, shellfish allergy has been diagnosed as a severe threat to human health over the past few years. Therefore, the detection of arginine kinase, known as the primary cause of shellfish, is vital for public health. For this aim, Zhou et al. (2020a, b) provided a fluorescence probe using fluorescence emission of synthesized carboxyl functionalized CDs and the quenching feature of GO and successfully achieved a detection limit of 0.14 ng/mL for sensing arginine kinase. In another food safety-related assay, Hu et al. (2021) used CDs provided by a one-pot green method in fluorescence-based sensing of *E. coli* in milk. As a donor fluorophore, CDs were modified with aptamer with specificity for *E. coli*. Additionally, they functionalized MNPs with DNA, which has a complementary strand of the *E. coli* aptamer. Incubating the target with CDs-MNPs conjugates led to reducing fluorescence intensity obtained from the fluorescent spectra of CDs, signifying signal-off sensing. In one recent experiment, Hu et al. (2019) developed AuNPs-CDs conjugate to detect melamine in milk. In the food industry, this nitrogen-based target is added illegally to raise apparent protein percentage in milk, which poses a threat to human health due to its combination with cyanuric acid. The detection limit

achieved in this assay was 3.6 nM. It is worth noting that increasing the amount of melamine incubated with the conjugation resulted in fluorescence intensity.

Another fluorescent NPs which have been widely utilized in providing fluorescence-based detection methods over recent years are silicon quantum dots (SiQDs). Besides being eco-friendly, highly soluble in common solvents, and biodegradable, they can be easily functionalized with other components that enhance their usage in sensing systems. In one experiment, SiQDs were produced by Wei et al. (2021) through a one-step method for sensing nitrite, a chemical compound which its immoderate amounts in food are damaging for human health. The capability of nitrite in quenching the fluorescence radiation emitted by these quantum dots owing to photoinduced electron transfer paves the way for target detection. With regard to the detection limit, they reached 25 nM in food samples. Moreover, molybdenum disulfide quantum dots (MoS₂ QDs) as fluorescent NPs are suitable for designing of detection platform in recent years. They exhibit fluorescent emission thanks to quantum confinement, and they are surface modifiable. To improve the fluorescence probe's sensitivity, the above-mentioned QDs can be modified with β -cyclodextrin (β -CD). This compound has some features such as hydrophilic exterior and hydrophobic internal space, which makes it a potential candidate for being used as a host in host-guest bindings. In one assay, Yi et al. (2021) provided a fluorescence probe by functionalizing MoS₂ QDs with β -CD to detect the analyte parathion-methyl (MP), an insecticide which its accumulation in food can cause harmful effects on human health. As can be seen in Fig. 1.3d, MoS₂ QDs were functionalized by 3-aminophenyl boronic acid (APBA) through amidation. It was followed by conjugating with β -CD to form a fluorescence probe. Additionally, the MP turned to p-nitrophenol through a hydrolysis reaction. Following this, p-nitrophenol developed complex with β -CD through host-guest binding, which led to effectual quenching of the fluorescence emitted from β -CD-MoS₂ QDs. Because the increase in MP concentration leads to a reduction in the intensity, target concentration can be accurately determined using this turn-off method.

Pieces of graphene at the nanoscale are named graphene quantum dots (GQDs). During the past decade, they have become a center of attention in developing sensing platforms, thanks to their characteristics, such as photoluminescence features. However, their quantum yields are noticeably lower than other fluorescent NPs. To undertake this barrier, scientists doped them with heteroatoms, including sulfur and nitrogen (Yang et al. 2015). As an example, a FRET-based detection approach was designed and provided by Nemati et al. (2018) for ethion sensing in the existence of Hg²⁺. This sensing system's target is a pesticide which its residue in food crops should be monitored to improve the safety of food. Mercury ions bind to the surface of S and N doped GQDs with a negative charge (act as a donor). Before the addition of ethion, Hg²⁺ quenched the fluorescence emission of the donor. After introducing the target, Hg²⁺ bound to ethion, which results in the recovery of N and S doped GQDs. The concentration of ethion could be accurately determined using the intensity change because of the target added to the system. It is worth mentioning that 8 mg/L's detection limit was achieved in this sensing-based assay. In Table 1.3,

Table 1.3 Application of sensing platforms in food safety utilizing fluorescent nanomaterials

Nanoparticle	Affinity agent	Target/S	Sensing principle	LOD	Real sample measurements	Ref
QDs and colloidal AuNPs	Monoclonal antibody	Sulfa quinoxaline	FRET	1 ng/mL	Yes, in foods	Hu et al. (2017)
H ₂ O ₂ -sensitive mercaptopropionic acid-modified CdTe QDs	Polyclonal antibody	<i>E. coli</i>	Fluorescence	5 × 10 ² CFU/mL	Yes, in real milk	Chen et al. (2016a, b)
CdSe/ZnS QDs	Molecularly imprinted polymer	N ϵ -carboxymethyl lysine	Fluorescence	2.6 μ g/L	Yes, in foods	Liu et al. (2016a, b, c)
QDs	Molecularly imprinted optopolymer	Tyramine	Fluorescence	7.0 μ g/kg	Yes, in fermented meat products	Zheng et al. (2019)
MNPs and QDs	Antibody	<i>E. coli</i>	Fluorescence	14 CFU/mL	Yes, in the spiked milk samples	Xue et al. (2018)
QD beads	Antibody	Zearalenone, ochratoxin A, and Fumonisin B1	Fluorescence	5, 20, and 10 ng/mL	Yes, in maize	Duan et al. (2019)
QDs and UCNPs	Monoclonal antibody	Norfloxacin	Fluorescence	2.5 μ g/L	Yes, in real milk	Hu et al. (2020a, b)
CdSe/ZnS QDs and AuNPs	Egg yolk antibody	Vibrio parahaemolyticus	Fluorescence	10 CFU/mL	Yes, in real marine food samples	Liu et al. (2017a, b)
QDs	Biomimetic antibody	Methyl parathion, chlorpyrifos, and trichlorfon	Fluorescence	0.21 ± 0.021, 0.44 ± 0.069, and 0.32 ± 0.033 μ g/L	Yes, in pear, carrot, kiwifruit, and banana samples	Jiang et al. (2019)
UCNPs	Monoclonal antibody	Sibutramine	Fluorescence	0.02 μ g/mL	Yes, in diet food samples	Zhang et al. (2020a, b)
UCNPs	Antibodies	<i>E. coli</i> and <i>Staphylococcus aureus</i>	Fluorescence	13 and 15 CFU/mL	Yes, in adulterated meat and milk samples	Zhang et al. (2017)

NaYF ₄ : Yb/Tm UCNPs	Antibody	Chloramphenicol	Fluorescence	0.01 pg/mL	Yes, in the muscle tissue, milk, and honey samples	Sheng et al. (2020)
Gold nanorods and UCNPs	Aptamer	Zearalenone and Fumonisin B1	Fluorescence	0.01 µg/L and 0.003 ng/L	Yes, in spiked corn samples	He et al. (2020)
UCNPs and magnetite-modified AuNPs	Aptamer	Lead (II)	FRET	5.7 nM	Yes, in tea and wastewater	Chen et al. (2020a, b)
Gold nanorods and UCNPs	Aptamer	Enterotoxin B	Fluorescence	0.9 pg/mL	Yes, in spiked milk samples	Wu et al. (2018a, b)
UCNPs and AuNPs	Imidacloprid antibody	Imidacloprid	Fluorescence	0.79 ng/mL	Yes, in spiked water, Chinese cabbage, and honey samples	Si et al. (2018)
UCNPs	Aptamer	Zearalenone	Fluorescence	0.126 µg/kg for corn and 0.007 µg/L for beer	Yes, in corn and beer	Wu et al. (2017)
MNPs conjugated with UCNPs	Aptamer	Enrofloxacin	Fluorescence	0.06 ng/mL	Yes, in food samples	Liu et al. (2016a, b)
UCNPs	Aptamer	Mercury ions, ochratoxin A, and <i>Salmonella</i>	Fluorescence	5 ppb, 3 ng/mL, and 85 CFU/mL	Yes, in real water samples	Jin et al. (2018)
UCNPs	Aptamer	<i>E. coli</i>	FRET	17 CFU/mL	Yes, in tap water and green tea powder	Wang et al. (2020a, b)
UCNPs	Aptamer	<i>E. coli</i>	FRET	3 CFU/mL	Yes, in tap/pond water, milk	Jin et al. (2017)
Magnetic and UCNPs	Aptamer	<i>E. coli</i>	Fluorescence	10 CFU/mL	Yes, in food	Li et al. (2020a)
Rare-earth doped UCNPs	Aptamer	Diazinon	FRET	0.023 ng/mL	Yes, in food	Rong et al. (2020)
UCNPs	Aptamer	Malathion	FRET	1.42 nM.	Yes, in food	Chen et al. (2020a, b)

(continued)

Table 1.3 (continued)

Nanoparticle	Affinity agent	Target/S	Sensing principle	LOD	Real sample measurements	Ref
UCNPs	Aptamer	AFBI	LRET	0.17 ng/mL	Yes, in food samples	Wang et al. (2019)
UCNPs	Anti-sulfa quinoxaline monoclonal antibody	Sulfa quinoxaline	Fluorescence	0.5 µg/kg	Yes, in animal-derived foods	Hu et al. (2016)
UCNPs	Polyacrylic acid	Fe ³⁺	Near-infrared luminescence	1 µM	Yes, in infant formula, milk powder	Zhang et al. (2019a, b)
NH ₂ -NaYF ₄ : Yb, Er/NaYF ₄ @SiO ₂ UCNPs	AuNPs	Cadmium ions	FRET	0.059 µM	Yes, in drinking water	Sun et al. (2020)
Au@Ag/graphene upconversion CDs	Aptamer	Hg ²⁺	Fluorescence	1 ppb	Yes, in food	Li et al. (2020b)
CDs		Acrylamide	Fluorescence	8.1 × 10 ⁻⁷ M	Yes, in artificially spiked white bread crust samples	Wei et al. (2020)
SiQDs		Potassium ferrocyanide	Fluorescence	30 ng/mL	Yes, in table salt and salted food samples	Na et al. (2019)
ZnO QDs	Vitamin B6 cofactors	Histamine	Fluorescence	0.59 µM and 0.97 µM	No	Yadav et al. (2020)
CDs	AuNPs	Aldicarb	Fluorescence	3.02 µg/L	Yes, in fruits and vegetables spiked sample	Sajwan et al. (2021)
Sulfur, chlorine, and nitrogen co-doped CDs		Manganese (VII)	Fluorescence	12.8 nM	Yes, in vegetable, cereal, and tea samples	Hu et al. (2020a, b)
Bluish green-emitting CDs		Curcumin	Fluorescence	28.7 nM	Yes, in dietary food samples	Liu et al. (2020a, b)
CDs		Ascorbic acid	Fluorescence	42 nM	Yes, in fresh fruits, vegetables, and commercial fruit juices samples	Liu et al. (2016a, b, c)

fluorescent NPs, affinity agents, target analytes, and the detection limit of each provided fluorescence-based sensor are represented.

1.5 Conclusion

The impact of nanoscience on the food industry cannot be neglected that it fulfills various requirements and contributes to undertaking the obstacles. Many articles in this field indicate the effective use of NPs in developing cost-effective, environmentally friendly sensors with high sensitivity and selectivity. Carbon-based and plasmonic/metallic NPs and fluorescent NPs, including QDs and UCNPs, are among the NPs which are useful for sensing food-related toxins, allergens, chemicals, pathogens, and enterotoxins over the past few years. Furthermore, aptamers and antibodies are salient examples of frequently used affinity agents for developing sensing platforms. Moveable analytic sensors with high efficiency can be developed to detect food-related analytes with considerably lower LODs in real samples. Most of these platforms possess great potential for highly selective multiplex sensing of more than one target simultaneously, which leads to time-saving detection of targets. The tables prepared in this chapter summarize NP-based sensing principles, food-related targets, and their detection limits, affinity agents, and applicability of methods for real sample measurements. Though sensing techniques which are based on nanoscience have numerous pros in comparison with other techniques, from many aspects such as LOD, and selectivity, their efficacious application in the above-mentioned field for various sorts of real sample measurements is still considered as a demanding issue because of the samples with complex nature and difficulties in sample separation steps. Developing robust and operational sample separation methods can significantly enhance the applicability of the detection techniques. Although these methods were assessed using real samples, only a few food samples were utilized for performance studies. However, using a diversity of real samples for sensing assays and comparing them with other conventional techniques can contribute to undertaking the issue as mentioned above. Other challenging issues are the intricate NP synthesis process along with costly precursors, which can be overcome by discovery of low-priced and efficient synthesis techniques. Additionally, some of the disease-causing pathogens cannot be noticed by available detection platforms due to the insufficiency of the detection agents. To conclude, the construction of novel, selective, multiplexed, and cost-effective sensing methods based on stable engineered NPs and target-specific affinity probes may revolutionize the field in near future.

References

Aghaie A, Khanmohammadi A, Hajian A, Schmid U, Bagheri H (2019) Nonenzymatic electrochemical determination of paraoxon ethyl in water and fruits by graphene-based NiFe bimetallic

- phosphosulfide nanocomposite as a superior sensing layer. *Food Anal Methods* 12(7): 1545–1555
- Alhabeab M, Maleski K, Anasori B, Lelyukh P, Clark L, Sin S, Gogotsi Y (2017) Guidelines for synthesis and processing of two-dimensional titanium carbide (Ti₃C₂T_x MXene). *Chem Mater* 29:7633–7644. <https://doi.org/10.1021/acs.chemmater.7b02847>
- Al-Nahain A, Lee JE, In I, Lee H, Lee KD, Jeong JH, Park SY (2013) Target delivery and cell imaging using hyaluronic acid-functionalized graphene quantum dots. *Mol Pharm* 10:3736–3744. <https://doi.org/10.1021/mp400219u>
- Annavam V, Chen M, Kutsanedzie FYH, Agyekum AA, Zareef M, Ahmad W, Hassan MM, Huanhuan L, Chen Q (2019) Synthesis of highly fluorescent RhDCP as an ideal inner filter effect pair for the NaYF₄:Yb,Er upconversion fluorescent nanoparticles to detect trace amount of Hg(II) in water and food samples. *J Photochem Photobiol A Chem* 382. <https://doi.org/10.1016/j.jphotochem.2019.111950>
- Arvand M, Mirroshandel AA (2019) An efficient fluorescence resonance energy transfer system from quantum dots to graphene oxide nano sheets: application in a photoluminescence aptasensing probe for the sensitive detection of diazinon. *Food Chem* 280:115–122. <https://doi.org/10.1016/j.foodchem.2018.12.069>
- Bao-Kai M, Mian L, Ling-Zhi C, Xin-Chu W, Cai S, Qing H (2020) Enzyme-MXene nanosheets: fabrication and application in electrochemical detection of H₂O₂. *J Inorg Mater* 35:132–138. <https://doi.org/10.15541/jim20190139>
- Bonilla JC, Bozkurt F, Ansari S, Sozer N, Kokini JL (2016) Applications of quantum dots in food science and biology. *Trends Food Sci Technol* 53:75–89. <https://doi.org/10.1016/j.tifs.2016.04.006>
- Bozkurt AG, Buyukgoz GG, Soforoglu M, Tamer U, Suludere Z, Boyaci IH (2018) Alkaline phosphatase labeled SERS active sandwich immunoassay for detection of *Escherichia coli*. *Spectrochim Acta Part A Mol Biomol Spectrosc* 194:8–13. <https://doi.org/10.1016/j.saa.2017.12.057>
- Caucheteur C, Guo T, Albert J (2015) Review of plasmonic fiber optic biochemical sensors: improving the limit of detection. *Anal Bioanal Chem* 407:3883–3897. <https://doi.org/10.1007/s00216-014-8411-6>
- Chandra P, Koh WCA, Noh HB, Shim YB (2012) In vitro monitoring of i-NOS concentrations with an immunosensor: The inhibitory effect of endocrine disruptors on i-NOS release. *Biosens Bioelectron*. <https://doi.org/10.1016/j.bios.2011.11.027>
- Chauhan R, Singh J, Sachdev T, Basu T, Malhotra BD (2016) Recent advances in mycotoxins detection. *Biosens Bioelectron* 81:532–545. <https://doi.org/10.1016/j.bios.2016.03.004>
- Chen J, Nugen SR (2019) Detection of protease and engineered phage-infected bacteria using peptide-graphene oxide nanosensors. *Anal Bioanal Chem* 411(12):2487–2492
- Chen L, Song J (2017) Tailored graphitic carbon nitride nanostructures: synthesis, modification, and sensing applications. *Adv Funct Mater*. <https://doi.org/10.1002/adfm.201702695>
- Chen J, Zhao JX (2012) Upconversion nanomaterials: Synthesis, mechanism, and applications in sensing. *Sensors* 12:2414–2435. <https://doi.org/10.3390/s120302414>
- Chen Z, Li G, Zhang L, Jiang J, Li Z, Peng Z, Deng L (2008) A new method for the detection of ATP using a quantum-dot-tagged aptamer. *Anal Bioanal Chem* 392:1185–1188. <https://doi.org/10.1007/s00216-008-2342-z>
- Chen H, Shao L, Li Q, Wang J (2013) Gold nanorods and their plasmonic properties. *Chem Soc Rev* 42:2679–2724. <https://doi.org/10.1039/C2CS35367A>
- Chen Q, Hu W, Sun C, Li H, Ouyang Q (2016a) Synthesis of improved upconversion nanoparticles as ultrasensitive fluorescence probe for mycotoxins. *Anal Chim Acta* 938:137–145. <https://doi.org/10.1016/j.aca.2016.08.003>
- Chen R, Huang X, Li J, Shan S, Lai W, Xiong Y (2016b) A novel fluorescence immunoassay for the sensitive detection of *Escherichia coli* O157:H7 in milk based on catalase-mediated fluorescence quenching of CdTe quantum dots. *Anal Chim Acta* 947:50–57. <https://doi.org/10.1016/j.aca.2016.10.017>

- Chen Q, Zhang L, Feng Y, Shi F, Wang Y, Wang P, Liu L (2018) Dual-functional peptide conjugated gold nanorods for the detection and photothermal ablation of pathogenic bacteria. *J Mater Chem B* 6:7643–7651. <https://doi.org/10.1039/C8TB01835A>
- Chen M, Hassan M, Li H, Chen Q (2020a) Fluorometric determination of lead(II) by using aptamer-functionalized upconversion nanoparticles and magnetite-modified gold nanoparticles. *Microchim Acta* 187. <https://doi.org/10.1007/s00604-019-4030-4>
- Chen Q, Sheng R, Wang P, Ouyang Q, Wang A, Ali S, Zareef M, Hassan MM (2020b) Ultra-sensitive detection of malathion residues using FRET-based upconversion fluorescence sensor in food. *Spectrochim. Acta - Part A Mol. Biomol. Spectrosc.* 241:118654. <https://doi.org/10.1016/j.saa.2020.118654>
- Choudhary M, Yadav P, Singh A, Kaur S, Ramirez-Vick J, Chandra P, Arora K, Singh SP (2016) CD 59 Targeted ultrasensitive electrochemical immunosensor for fast and noninvasive diagnosis of oral cancer. *Electroanalysis* 28:2565–2574. <https://doi.org/10.1002/elan.201600238>
- Danielson E, Dindo M, Porkovich AJ, Kumar P, Wang Z, Jain P, Mete T, Ziadi Z, Kikkeri R, Laurino P, Sowwan M (2020) Non-enzymatic and highly sensitive lactose detection utilizing graphene field-effect transistors. *Biosens Bioelectron* 165:112419. <https://doi.org/10.1016/j.bios.2020.112419>
- Deka S, Saxena V, Hasan A, Chandra P, Pandey LM (2018) Synthesis, characterization and in vitro analysis of α -Fe₂O₃-GdFeO₃ biphasic materials as therapeutic agent for magnetic hyperthermia applications. *Mater Sci Eng C* 92:932–941. <https://doi.org/10.1016/j.msec.2018.07.042>
- Du J, Singh H, Dong W, Bai Y, Yi T-H (2018) Colorimetric detection of *Listeria monocytogenes* using one-pot biosynthesized flower-shaped gold nanoparticles. *Sensors Actuators B Chem* 265:285–292. <https://doi.org/10.1016/j.snb.2018.03.067>
- Duan N, Shen M, Wu S, Zhao C, Ma X, Wang Z (2017) Graphene oxide wrapped Fe₃O₄@Au nanostructures as substrates for aptamer-based detection of *Vibrio parahaemolyticus* by surface-enhanced Raman spectroscopy. *Microchim Acta* 184:2653–2660. <https://doi.org/10.1007/s00604-017-2298-9>
- Duan H, Li Y, Shao Y, Huang X, Xiong Y (2019) Multicolor quantum dot nanobeads for simultaneous multiplex immunochromatographic detection of mycotoxins in maize. *Sensors Actuators B Chem* 291:411–417. <https://doi.org/10.1016/j.snb.2019.04.101>
- Duan N, Shen M, Qi S, Wang W, Wu S, Wang Z (2020) A SERS aptasensor for simultaneous multiple pathogens detection using gold decorated PDMS substrate. *Spectrochim Acta Part A Mol Biomol Spectrosc* 230:118103. <https://doi.org/10.1016/j.saa.2020.118103>
- Erdogan ZO, Akin I, Kucukkolbasi S (2018) A new non-enzymatic sensor based on TiO₂-Ag/polypyrrole for electrochemical detection of tyramine. *Synth Met* 246:96–100. <https://doi.org/10.1016/j.synthmet.2018.10.006>
- Fu L, Xie K, Wu D, Wang A, Zhang H, Ji Z (2020) Electrochemical determination of vanillin in food samples by using pyrolyzed graphitic carbon nitride. *Mater Chem Phys* 242:122462. <https://doi.org/10.1016/j.matchemphys.2019.122462>
- Gao N, He C, Ma M, Cai Z, Zhou Y, Chang G, Wang X, He Y (2019) Electrochemical co-deposition synthesis of Au-ZrO₂-graphene nanocomposite for a nonenzymatic methyl parathion sensor. *Anal Chim Acta* 1072:25–34. <https://doi.org/10.1016/j.aca.2019.04.043>
- Govindasamy M, Mani V, Chen S, Chen T (2017) Methyl parathion detection in vegetables and fruits using silver @ graphene nanoribbons nanocomposite modified screen printed electrode. *Nat Publ Gr*:1–11. <https://doi.org/10.1038/srep46471>
- Guo J, Li Y, Wang L, Xu J, Huang Y, Luo Y, Shen F, Sun C, Meng R (2016) Aptamer-based fluorescent screening assay for acetamiprid via inner filter effect of gold nanoparticles on the fluorescence of CdTe quantum dots. *Anal Bioanal Chem* 408:557–566. <https://doi.org/10.1007/s00216-015-9132-1>
- Guo P, Yang W, Hu H, Wang Y, Li P (2019) Rapid detection of aflatoxin B 1 by dummy template molecularly imprinted polymer capped CdTe quantum dots. *Anal Bioanal Chem* 411(12):2607–2617. <https://doi.org/10.1007/s00216-019-01708-2>

- Gupta BD, Pathak A, Semwal V (2019) Carbon-based nanomaterials for plasmonic sensors: a review. *Sensors (Switzerland)* 19. <https://doi.org/10.3390/s19163536>
- Haase M, Schäfer H (2011) Upconverting nanoparticles. *Angew Chem: Int Ed* 50:5808–5829. <https://doi.org/10.1002/anie.201005159>
- Hassan MM, Zareef M, Jiao T, Liu S, Xu Y, Viswadevarayalu A, Li H, Chen Q (2021) Signal optimized rough silver nanoparticle for rapid SERS sensing of pesticide residues in tea. *Food Chem* 338:127796. <https://doi.org/10.1016/j.foodchem.2020.127796>
- He Q, Liu J, Liu X, Xia Y, Li G, Deng P, Chen D (2018) Novel electrochemical sensors based on cuprous oxide-electrochemically reduced graphene oxide nanocomposites modified electrode toward sensitive detection of sunset yellow. *Molecules* 23(9):2130. <https://doi.org/10.3390/molecules23092130>
- He D, Wu Z, Cui B, Xu E, Jin Z (2019) Establishment of a dual mode immunochromatographic assay for *Campylobacter jejuni* detection. *Food Chem* 289:708–713. <https://doi.org/10.1016/j.foodchem.2019.03.106>
- He D, Wu Z, Cui B, Jin Z, Xu E (2020) A fluorometric method for aptamer-based simultaneous determination of two kinds of the fusarium mycotoxins zearalenone and fumonisin B1 making use of gold nanorods and upconversion nanoparticles. *Microchim Acta* 187(4):1–8. <https://doi.org/10.1007/s00604-020-04236-4>
- Heo NS, Oh SY, Ryu MY, Baek SH, Park TJ, Choi C, Huh YS, Park JP (2019) Affinity peptide-guided plasmonic biosensor for detection of noroviral protein and human norovirus. *Biotechnol Bioprocess Eng* 24:318–325. <https://doi.org/10.1007/s12257-018-0410-6>
- Hu G, Sheng W, Zhang Y, Wang J, Wu X, Wang S (2016) Upconversion nanoparticles and monodispersed magnetic polystyrene microsphere based fluorescence immunoassay for the detection of sulfaquinolone in animal-derived foods. *J Agric Food Chem* 64:3908–3915. <https://doi.org/10.1021/acs.jafc.6b01497>
- Hu G, Sheng W, Li J, Zhang Y, Wang J, Wang S (2017) Fluorescent quenching immune chromatographic strips with quantum dots and upconversion nanoparticles as fluorescent donors for visual detection of sulfaquinolone in foods of animal origin. *Anal Chim Acta* 982:185–192. <https://doi.org/10.1016/j.aca.2017.06.013>
- Hu X, Shi J, Shi Y, Zou X, Arslan M, Zhang W, Huang X, Li Z, Xu Y (2019) Use of a smartphone for visual detection of melamine in milk based on Au@Carbon quantum dots nanocomposites. *Food Chem* 272:58–65. <https://doi.org/10.1016/j.foodchem.2018.08.021>
- Hu G, Gao S, Han X, Yang L (2020a) Comparison of immunochromatographic strips using colloidal gold, quantum dots, and upconversion nanoparticles for visual detection of norfloxacin in milk samples. *Food Anal Methods* 13:1069–1077. <https://doi.org/10.1007/s12161-020-01725-3>
- Hu Q, Liu LF, Sun H, Han J, Gong X, Liu L, Yang ZQ (2020b) An ultra-selective fluorescence method with enhanced sensitivity for the determination of manganese (VII) in food stuffs using carbon quantum dots as nanoprobe. *J Food Compos Anal* 88:103447. <https://doi.org/10.1016/j.jfca.2020.103447>
- Hu X, Li Y, Xu Y, Gan Z, Zou X, Shi J, Huang X, Li Z, Li Y (2021) Green one-step synthesis of carbon quantum dots from orange peel for fluorescent detection of *Escherichia coli* in milk. *Food Chem* 339:127775. <https://doi.org/10.1016/j.foodchem.2020.127775>
- Hua R, Hao N, Lu J, Qian J, Liu Q, Li H, Wang K (2018) A sensitive potentiometric resolved ratiometric photoelectrochemical aptasensor for *Escherichia coli* detection fabricated with non-metallic nanomaterials. *Biosens Bioelectron* 106:57–63. <https://doi.org/10.1016/j.bios.2018.01.053>
- Jelinek R (2017) Carbon quantum dots. synthesis, properties and applications
- Jiang M, He J, Gong J, Gao H, Xu Z (2019) Development of a quantum dot-labelled biomimetic fluorescence immunoassay for the simultaneous determination of three organophosphorus pesticide residues in agricultural products. *Food Agric Immunol* 30:248–261. <https://doi.org/10.1080/09540105.2019.1572714>

- Jin D, Xu Q, Yu L, Mao A, Hu X (2016) A novel sensor for the detection of acetamiprid in vegetables based on its photocatalytic degradation compound. *Food Chem* 194:959–965. <https://doi.org/10.1016/j.foodchem.2015.08.118>
- Jin B, Wang S, Lin M, Jin Y, Zhang S, Cui X, Gong Y, Li A, Xu F, Lu TJ (2017) Upconversion nanoparticles based FRET aptasensor for rapid and ultrasensitive bacteria detection. *Biosens Bioelectron* 90:525–533. <https://doi.org/10.1016/j.bios.2016.10.029>
- Jin B, Yang Y, He R, Park YI, Lee A, Bai D, Li F, Lu TJ, Xu F, Lin M (2018) Lateral flow aptamer assay integrated smartphone-based portable device for simultaneous detection of multiple targets using upconversion nanoparticles. *Sensors Actuators B Chem* 276:48–56. <https://doi.org/10.1016/j.snb.2018.08.074>
- Kahraman M, Mullen ER, Korkmaz A, Wachsmann-Hogiu S (2017) Fundamentals and applications of SERS-based bioanalytical sensing. *Nano* 6:831–852. <https://doi.org/10.1515/nanoph-2016-0174>
- Karthik R, Kumar JV, Chen SM, Kokulnathan T, Chen TW, Sakthianathan S, Chiu TW, Muthuraj V (2018) Development of novel 3D flower-like praseodymium molybdate decorated reduced graphene oxide: an efficient and selective electrocatalyst for the detection of acetylcholinesterase inhibitor methyl parathion. *Sensors Actuators B Chem* 270:353–361. <https://doi.org/10.1016/j.snb.2018.05.054>
- Kaushal S, Priyadarshi N, Pinnaka AK, Soni S, Deep A, Singhal NK (2019) Glycoconjugates coated gold nanorods based novel biosensor for optical detection and photothermal ablation of food borne bacteria. *Sensors Actuators B Chem* 289:207–215. <https://doi.org/10.1016/j.snb.2019.03.096>
- Khan R, Andreescu S (2020) MXenes-based bioanalytical sensors: design, characterization, and applications. *Sensors* 20:5434. <https://doi.org/10.3390/s20185434>
- Khateb H, Klös G, Meyer RL, Sutherland DS (2020) Development of a Label-Free LSPR-Apta sensor for *Staphylococcus aureus* detection. *ACS Appl Bio Mater* 3:3066–3077. <https://doi.org/10.1021/acsaabm.0c00110>
- Kurt H, Eyüpoğlu AE, Sütlü T, Budak H, Yüce M (2019) Plasmonic selection of ssDNA Aptamers against fibroblast growth factor receptor. *ACS Comb Sci* 21:578–587. <https://doi.org/10.1021/acscmbosci.9b00059>
- Lee S, Jun B-H (2019) Silver nanoparticles: synthesis and application for nanomedicine. *Int J Mol Sci* 20:865. <https://doi.org/10.3390/ijms20040865>
- Li M, Chen T, Gooding JJ, Liu J (2019) Review of carbon and graphene quantum dots for sensing. *ACS Sensors* 4:1732–1748. <https://doi.org/10.1021/acssensors.9b00514>
- Li L, Zhang H, Song D, Xu K, Zheng Y, Xiao H, Liu Y, Li J, Song X (2020a) Simultaneous detection of three zoonotic pathogens based on phage display peptide and multicolor quantum dots. *Anal Biochem* 608:113854. <https://doi.org/10.1016/j.ab.2020.113854>
- Li Y, Lu C, Zhou S, Fauconnier M-L, Gao F, Fan B, Lin J, Wang F, Zheng J (2020b) Sensitive and simultaneous detection of different pathogens by surface-enhanced Raman scattering based on aptamer and Raman reporter co-mediated gold tags. *Sensors Actuators B Chem* 317:128182. <https://doi.org/10.1016/j.snb.2020.128182>
- Li H, Ahmad W, Rong Y, Chen Q, Zuo M, Ouyang Q, Guo Z (2020c) Designing an aptamer based magnetic and upconversion nanoparticles conjugated fluorescence sensor for screening *Escherichia coli* in food. *Food Control* 107:106761. <https://doi.org/10.1016/j.foodcont.2019.106761>
- Li H, Huang X, Mehedi Hassan M, Zuo M, Wu X, Chen Y, Chen Q (2020d) Dual-channel biosensor for Hg²⁺ sensing in food using Au@Ag/graphene-upconversion nanohybrids as metal-enhanced fluorescence and SERS indicators. *Microchem J* 154:104563. <https://doi.org/10.1016/j.microc.2019.104563>
- Lin B, Yu Y, Li R, Cao Y, Guo M (2016) Turn-on sensor for quantification and imaging of acetamiprid residues based on quantum dots functionalized with aptamer. *Sensors Actuators B Chem* 229:100–109. <https://doi.org/10.1016/j.snb.2016.01.114>

- Liu H, Wu D, Zhou K, Wang J, Sun B (2016a) Development and applications of molecularly imprinted polymers based on hydrophobic CdSe/ZnS quantum dots for optosensing of N- ϵ -carboxymethyllysine in foods. *Food Chem* 211:34–40. <https://doi.org/10.1016/j.foodchem.2016.05.038>
- Liu J, Chen Y, Wang W, Feng J, Liang M, Ma S, Chen X (2016b) “switch-On” Fluorescent sensing of ascorbic acid in food samples based on carbon quantum dots-MnO₂ Probe. *J Agric Food Chem* 64:371–380. <https://doi.org/10.1021/acs.jafc.5b05726>
- Liu X, Su L, Zhu L, Gao X, Wang Y, Bai F, Tang Y, Li J (2016c) Hybrid material for enrofloxacin sensing based on aptamer-functionalized magnetic nanoparticle conjugated with upconversion nanoprobles. *Sensors Actuators B Chem* 233:394–401. <https://doi.org/10.1016/j.snb.2016.04.096>
- Liu Y, Liu X, Guo Z, Hu Z, Xue Z, Lu X (2017a) Horseradish peroxidase supported on porous graphene as a novel sensing platform for detection of hydrogen peroxide in living cells sensitively. *Biosens Bioelectron* 87:101–107. <https://doi.org/10.1016/j.bios.2016.08.015>
- Liu Y, Zhao C, Fu K, Song X, Xu K, Wang J, Li J (2017b) Selective turn-on fluorescence detection of *Vibrio parahaemolyticus* in food based on charge-transfer between CdSe/ZnS quantum dots and gold nanoparticles. *Food Control* 80:380–387. <https://doi.org/10.1016/j.foodcont.2017.05.032>
- Liu J, He H, Xiao D, Yin S, Ji W, Jiang S, Luo D, Wang B, Liu Y (2018a) Recent advances of plasmonic nanoparticles and their applications. *Materials (Basel)* 11. <https://doi.org/10.3390/ma11101833>
- Liu JM, Hu Y, Yang YK, Liu H, Fang GZ, Lu X, Wang S (2018b) Emerging functional nanomaterials for the detection of food contaminants. *Trends Food Sci Technol*. <https://doi.org/10.1016/j.tifs.2017.11.005>
- Liu Y, Wang J, Zhao C, Guo X, Song X, Zhao W, Liu S, Xu K, Li J (2019) A multicolorimetric assay for rapid detection of *Listeria monocytogenes* based on the etching of gold nanorods. *Anal Chim Acta* 1048:154–160. <https://doi.org/10.1016/j.aca.2018.10.020>
- Liu J, Jalali M, Mahshid S, Wachsmann-Hogiu S (2020a) Are plasmonic optical biosensors ready for use in point-of-need applications? *Analyst* 145:364–384. <https://doi.org/10.1039/C9AN02149C>
- Liu L, Hu Q, Sun H, Han J, Pan Y, Yang ZQ (2020b) An ultra-sensitive analytical platform based on bluish green emitting carbon quantum dots for the detection of curcumin in dietary foods. *J Food Compos Anal* 94:103639. <https://doi.org/10.1016/j.jfca.2020.103639>
- Loiseau A, Asila V, Boitel-Aullen G, Lam M, Salmain M, Boujday S (2019a) Silver-based plasmonic nanoparticles for and their use in biosensing. *Biosensors* 9:78. <https://doi.org/10.3390/bios9020078>
- Loiseau A, Zhang L, Hu D, Salmain M, Mazouzi Y, Flack R, Liedberg B, Boujday S (2019b) Core-shell gold/silver nanoparticles for localized surface plasmon resonance-based naked-eye toxin biosensing. *ACS Appl Mater Interfaces* 11:46462–46471. <https://doi.org/10.1021/acsami.9b14980>
- Ma X, Xu X, Xia Y, Wang Z (2018) SERS aptasensor for *Salmonella typhimurium* detection based on spiny gold nanoparticles. *Food Control* 84:232–237. <https://doi.org/10.1016/j.foodcont.2017.07.016>
- Magesa F, Wu Y, Tian Y, Vianney J-MM, Buza J, He Q, Tan Y (2019) Graphene and graphene like 2D graphitic carbon nitride: electrochemical detection of food colorants and toxic substances in environment. *Trends Environ Anal Chem* 23:e00064. <https://doi.org/10.1016/j.teac.2019.e00064>
- Mahato K, Kumar S, Srivastava A, Maurya PK, Singh R, Chandra P (2018) Electrochemical immunoassays: fundamentals and applications in clinical diagnostics. In: *Handbook of immunoassay technologies*. <https://doi.org/10.1016/B978-0-12-811762-0.00014-1>
- Mansoori B, Shotorbani SS, Baradaran B (2014) RNA interference and its role in cancer therapy. *Adv Pharm Bull* 4:313–321. <https://doi.org/10.5681/apb.2014.046>

- Masdor N, Altintas Z, Tothill I (2017) Surface plasmon resonance immunosensor for the detection of *Campylobacter jejuni*. *Chemosensors* 5:16. <https://doi.org/10.3390/chemosensors5020016>
- Matea CT, Mocan T, Tabaran F, Pop T, Mosteanu O, Puia C, Iancu C, Mocan L (2017) Quantum dots in imaging, drug delivery and sensor applications. *Int J Nanomedicine* 12:5421–5431. <https://doi.org/10.2147/IJN.S138624>
- McElwain TF, Thumbi SM (2017) Animal pathogens and their impact on animal health, the economy, food security, food safety and public health. *OIE Rev Sci Tech* 36:423–433. <https://doi.org/10.20506/rst.36.2.2663>
- Mishra GK, Barfidokht A, Tehrani F, Mishra RK (2018) Food safety analysis using electrochemical biosensors. *Foods*. <https://doi.org/10.3390/foods7090141>
- Molaei MJ (2019) Carbon quantum dots and their biomedical and therapeutic applications: a review. *RSC Adv* 9:6460–6481. <https://doi.org/10.1039/c8ra08088g>
- Na M, Chen Y, Han Y, Ma S, Liu J, Chen X (2019) Determination of potassium ferrocyanide in table salt and salted food using a water-soluble fluorescent silicon quantum dots. *Food Chem* 288:248–255. <https://doi.org/10.1016/j.foodchem.2019.02.111>
- Naguib M, Kurtoglu M, Presser V, Lu J, Niu J, Heon M, Hultman L, Gogotsi Y, Barsoum MW (2011) Two-dimensional nanocrystals produced by exfoliation of Ti 3AlC 2. *Adv Mater* 23: 4248–4253. <https://doi.org/10.1002/adma.201102306>
- Nehra M, Dilbaghi N, Hassan AA, Kumar S (2019) Carbon-based nanomaterials for the development of sensitive nanosensor platforms. In: *Advances in nanosensors for biological and environmental analysis*. Elsevier, pp 1–25. <https://doi.org/10.1016/b978-0-12-817456-2.00001-2>
- Nemati F, Hosseini M, Zare-Dorabei R, Ganjali MR (2018) Sensitive recognition of ethion in food samples using turn-on fluorescence N and S co-doped graphene quantum dots. *Anal Methods* 10:1760–1766. <https://doi.org/10.1039/c7ay02850d>
- Novoselov KS, Geim AK, Morozov SV, Jiang D, Zhang Y, Dubonos SV, Grigorieva IV, Firsov AA (2004) Electric field effect in atomically thin carbon films. *Science* (80-) 306:666–669. <https://doi.org/10.1126/science.1102896>
- Nsibandé SA, Forbes PBC (2016) Fluorescence detection of pesticides using quantum dot materials – a review. *Anal Chim Acta* 945:9–22. <https://doi.org/10.1016/j.aca.2016.10.002>
- Oh SY, Heo NS, Shukla S, Cho H-J, Vilian ATE, Kim J, Lee SY, Han Y-K, Yoo SM, Huh YS (2017) Development of gold nanoparticle-aptamer-based LSPR sensing chips for the rapid detection of *Salmonella typhimurium* in pork meat. *Sci Rep* 7:10130. <https://doi.org/10.1038/s41598-017-10188-2>
- Pan M, Yin Z, Liu K, Du X, Liu H, Wang S (2019) Carbon-based nanomaterials in sensors for food safety. *Nano*. <https://doi.org/10.3390/nano9091330>
- Pang B, Zheng Y, Wang J, Liu Y, Song X, Li J, Yao S, Fu K, Xu K, Zhao C, Li J (2019) Colorimetric detection of *Staphylococcus aureus* using gold nanorods labeled with yolk immunoglobulin and urease, magnetic beads, and a phenolphthalein impregnated test paper. *Microchim Acta* 186:611. <https://doi.org/10.1007/s00604-019-3722-0>
- Parate K, Pola CC, Rangnekar SV, Mendivelso-Perez DL, Smith EA, Hersam MC, Gomes CL, Claussen JC (2020) Aerosol-jet-printed graphene electrochemical histamine sensors for food safety monitoring. *2D Mater* 7(3):034002. <https://doi.org/10.1088/2053-1583/ab8919>
- Park BJ, Hong AR, Park S, Kyung KU, Lee K, Jang HS (2017) Flexible transparent displays based on core/shell upconversion nanophosphor-incorporated polymer waveguides. *Sci Rep* 7:1–11. <https://doi.org/10.1038/srep45659>
- Pehlivan ZS, Torabfam M, Kurt H, Ow-Yang C, Hildebrandt N, Yüce M (2019) Aptamer and nanomaterial based FRET biosensors: a review on recent advances (2014–2019). *Microchim Acta* 186:563. <https://doi.org/10.1007/s00604-019-3659-3>
- Quintela IA, de los Reyes BG, Lin C-S, Wu VCH (2019) Simultaneous colorimetric detection of a variety of *Salmonella* spp. in food and environmental samples by optical biosensing using oligonucleotide-gold nanoparticles. *Front Microbiol* 10:1–12. <https://doi.org/10.3389/fmicb.2019.01138>

- Ramalingam M, Ponnusamy VK, Sangilimuthu SN (2019) A nanocomposite consisting of porous graphitic carbon nitride nanosheets and oxidized multiwalled carbon nanotubes for simultaneous stripping voltammetric determination of cadmium(II), mercury(II), lead(II) and zinc(II). *Microchim Acta* 186:69. <https://doi.org/10.1007/s00604-018-3178-7>
- Ren W, Ballou DR, FitzGerald R, Irudayaraj J (2019) Plasmonic enhancement in lateral flow sensors for improved sensing of *E. coli* O157:H7. *Biosens Bioelectron* 126:324–331. <https://doi.org/10.1016/j.bios.2018.10.066>
- Reshma VG, Mohanan PV (2019) Quantum dots: applications and safety consequences. *J Lumin* 205:287–298. <https://doi.org/10.1016/j.jlumin.2018.09.015>
- Rodríguez-Lorenzo L, Garrido-Maestu A, Bhunia AK, Espiña B, Prado M, Diéguez L, Abalde-Cela S (2019) Gold nanostars for the detection of foodborne pathogens via surface-enhanced Raman scattering combined with microfluidics. *ACS Appl Nano Mater* 2:6081–6086. <https://doi.org/10.1021/acsanm.9b01223>
- Rong Y, Li H, Ouyang Q, Ali S, Chen Q (2020) Rapid and sensitive detection of diazinon in food based on the FRET between rare-earth doped upconversion nanoparticles and graphene oxide. *Spectrochim Acta: Part A Mol Biomol Spectrosc* 239:118500. <https://doi.org/10.1016/j.saa.2020.118500>
- Rouhani M (2019) Fluoro-functionalized graphene as a promising nanosensor in detection of fish spoilage: a theoretical study. *Chem Phys Lett* 719:91–102. <https://doi.org/10.1016/j.cplett.2019.02.001>
- Rozmysłowska-Wojciechowska A, Karwowska E, Poźniak S, Wojciechowski T, Chlubny L, Olszyna A, Ziemkowska W, Jastrzębska AM (2019) Influence of modification of Ti3C2 MXene with ceramic oxide and noble metal nanoparticles on its antimicrobial properties and ecotoxicity towards selected algae and higher plants. *RSC Adv* 9:4092–4105. <https://doi.org/10.1039/C8RA07633B>
- Sajwan RK, Lakshmi GBVS, Solanki PR (2021) Fluorescence tuning behavior of carbon quantum dots with gold nanoparticles via novel intercalation effect of aldarcarb. *Food Chem* 340:127835. <https://doi.org/10.1016/j.foodchem.2020.127835>
- Shams S, Bakhshi B, Tohidi Moghadam T, Behmanesh M (2019) A sensitive gold-nanorods-based nanobiosensor for specific detection of *Campylobacter jejuni* and *Campylobacter coli*. *J Nanobiotechnology* 17:43. <https://doi.org/10.1186/s12951-019-0476-0>
- Sharma R, Raghavarao KSMS (2018) Nanoparticle-based aptasensors for food contaminant detection, nanomaterials for food applications. Elsevier Inc. <https://doi.org/10.1016/B978-0-12-814130-4.00006-3>
- Shen Q, Jin R, Xue J, Lu Y, Dai Z (2016) Analysis of trace levels of sulfonamides in fish tissue using micro-scale pipette tip-matrix solid-phase dispersion and fast liquid chromatography tandem mass spectrometry. *Food Chem* 194:508–515. <https://doi.org/10.1016/j.foodchem.2015.08.050>
- Sheng W, Shi Y, Ma J, Wang L, Zhang B, Chang Q, Duan W, Wang S (2019) Highly sensitive atrazine fluorescence immunoassay by using magnetic separation and upconversion nanoparticles as labels. *Microchim Acta*:186. <https://doi.org/10.1007/s00604-019-3667-3>
- Sheng W, Huang N, Liu Y, Zhang B, Zhang W, Wang S (2020) An ultrasensitive fluorescence immunoassay based on magnetic separation and upconversion nanoparticles as labels for the detection of chloramphenicol in animal-derived foods. *Food Anal Methods* 13(11):2039–2049. <https://doi.org/10.1007/s12161-020-01820-5>
- Si F, Zou R, Jiao S, Qiao X, Guo Y, Zhu G (2018) Inner filter effect-based homogeneous immunoassay for rapid detection of imidacloprid residue in environmental and food samples. *Ecotoxicol Environ Saf* 148:862–868. <https://doi.org/10.1016/j.ecoenv.2017.11.062>
- Song L, Zhang L, Huang Y, Chen L, Zhang G, Shen Z, Zhang J, Xiao Z, Chen T (2017) Amplifying the signal of localized surface plasmon resonance sensing for the sensitive detection of *Escherichia coli* O157:H7. *Sci Rep* 7:3288. <https://doi.org/10.1038/s41598-017-03495-1>
- Sullivan JJ, Goh KS (2000) Evaluation and validation of a commercial ELISA for diazinon in surface waters. *J Agric Food Chem* 48:4071–4078. <https://doi.org/10.1021/jf000432t>

- Sun L, Wang T, Sun Y, Li Z, Song H, Zhang B, Zhou G, Zhou H, Hu J (2020) Fluorescence resonance energy transfer between $\text{NH}_2\text{-NaYF}_4\text{:Yb,Er/NaYF}_4\text{/SiO}_2$ upconversion nanoparticles and gold nanoparticles for the detection of glutathione and cadmium ions. *Talanta* 207:120294. <https://doi.org/10.1016/j.talanta.2019.120294>
- Szuplewska A, Kulpińska D, Dybko A, Chudy M, Jastrzębska AM, Olszyna A, Brzózka Z (2020) Future applications of MXenes in biotechnology, nanomedicine, and sensors. *Trends Biotechnol.* <https://doi.org/10.1016/j.tibtech.2019.09.001>
- Tabrizi MA, Shamsipur M, Saber R, Sarkar S, Ebrahimi V (2017) A high sensitive visible light-driven photoelectrochemical aptasensor for shrimp allergen tropomyosin detection using graphitic carbon nitride-TiO₂ nanocomposite. *Biosens Bioelectron* 98:113–118. <https://doi.org/10.1016/j.bios.2017.06.040>
- Takemura K, Lee J, Suzuki T, Hara T, Abe F, Park EY (2019) Ultrasensitive detection of norovirus using a magnetofluoroimmunoassay based on synergic properties of gold/magnetic nanoparticle hybrid nanocomposites and quantum dots. *Sensors Actuators B Chem* 296:126672. <https://doi.org/10.1016/j.snb.2019.126672>
- Vanegas D, Patiño L, Mendez C, Oliveira D, Torres A, Gomes C, McLamore E (2018) Laser scribed graphene biosensor for detection of biogenic amines in food samples using locally sourced materials. *Biosensors* 8:42. <https://doi.org/10.3390/bios8020042>
- Verma S, Choudhary J, Singh KP, Chandra P, Singh SP (2019) Uricase grafted nanoconducting matrix based electrochemical biosensor for ultrafast uric acid detection in human serum samples. *Int J Biol Macromol.* <https://doi.org/10.1016/j.ijbiomac.2019.02.121>
- Wagner AM, Knipe JM, Orive G, Peppas NA (2019) Quantum dots in biomedical applications. *Acta Biomater* 94:44–63. <https://doi.org/10.1016/j.actbio.2019.05.022>
- Wang B, Park B (2020) Immunoassay biosensing of foodborne pathogens with surface plasmon resonance imaging: a review. *J Agric Food Chem.* <https://doi.org/10.1021/acs.jafc.0c02295>
- Wang Z, Wu S, Colombi Ciacchi L, Wei G (2018) Graphene-based nanoplatforms for surface-enhanced Raman scattering sensing. *Analyst* 143:5074–5089. <https://doi.org/10.1039/c8an01266k>
- Wang F, Han Y, Wang S, Ye Z, Wei L, Xiao L (2019) Single-particle LRET Aptasensor for the sensitive detection of Aflatoxin B1 with upconversion nanoparticles. *Anal Chem* 91:11856–11863. <https://doi.org/10.1021/acs.analchem.9b02599>
- Wang G, Sun J, Yao Y, An X, Zhang H, Chu G, Jiang S, Guo Y, Sun X, Liu Y (2020a) Detection of Inosine Monophosphate (IMP) in meat using double-enzyme sensor. *Food Anal Methods* 13: 420–432. <https://doi.org/10.1007/s12161-019-01652-y>
- Wang P, Wang A, Hassan MM, Ouyang Q, Li H, Chen Q (2020b) A highly sensitive upconversion nanoparticles-WS₂ nanosheet sensing platform for *Escherichia coli* detection. *Sensors Actuators B Chem* 320:128434. <https://doi.org/10.1016/j.snb.2020.128434>
- Wei C, Li M, Zhao X (2018) Surface-enhanced Raman Scattering (SERS) with silver nano substrates synthesized by microwave for rapid detection of foodborne pathogens. *Front Microbiol* 9:1–9. <https://doi.org/10.3389/fmicb.2018.02857>
- Wei Q, Liu T, Pu H, Sun DW (2020) Determination of acrylamide in food products based on the fluorescence enhancement induced by distance increase between functionalized carbon quantum dots. *Talanta* 218:121152. <https://doi.org/10.1016/j.talanta.2020.121152>
- Wei N, Wei MX, Huang BH, Guo XF, Wang H (2021) One-pot facile synthesis of green-emitting fluorescent silicon quantum dots for the highly selective and sensitive detection of nitrite in food samples. *Dyes Pigments* 184:108848. <https://doi.org/10.1016/j.dyepig.2020.108848>
- Wen S, Zhou J, Zheng K, Bednarkiewicz A, Liu X, Jin D (2018) Advances in highly doped upconversion nanoparticles. *Nat Commun* 9:2415. <https://doi.org/10.1038/s41467-018-04813-5>
- Wilhelm S (2017) Perspectives for upconverting nanoparticles. *ACS Nano* 11:10644–10653. <https://doi.org/10.1021/acs.nano.7b07120>

- Wu Z (2019) Simultaneous detection of *Listeria monocytogenes* and *Salmonella typhimurium* by a SERS-based lateral flow immunochromatographic assay. *Food Anal Methods* 12:1086–1091. <https://doi.org/10.1007/s12161-019-01444-4>
- Wu Z, Xu E, Chughtai MFJ, Jin Z, Irudayaraj J (2017) Highly sensitive fluorescence sensing of zearealenone using a novel aptasensor based on upconverting nanoparticles. *Food Chem* 230: 673–680. <https://doi.org/10.1016/j.foodchem.2017.03.100>
- Wu L, Lu X, Dhanjai, Wu ZS, Dong Y, Wang X, Zheng S, Chen J (2018a) 2D transition metal carbide MXene as a robust biosensing platform for enzyme immobilization and ultrasensitive detection of phenol. *Biosens Bioelectron* 107:69–75. <https://doi.org/10.1016/j.bios.2018.02.021>
- Wu Z, He D, Cui B (2018b) A fluorometric assay for staphylococcal enterotoxin B by making use of platinum coated gold nanorods and of upconversion nanoparticles. *Microchim Acta* 185:1–8. <https://doi.org/10.1007/s00604-018-3058-1>
- Xie H, Li P, Shao J, Huang H, Chen Y, Jiang Z, Chu PK, Yu XF (2019) Electrostatic self-assembly of Ti3C2Tx MXene and gold nanorods as an efficient surface-enhanced Raman scattering platform for reliable and high-sensitivity determination of organic pollutants. *ACS Sensors* 4: 2303–2310. <https://doi.org/10.1021/acssensors.9b00778>
- Xiong Y, Pei K, Wu Y, Duan H, Lai W, Xiong Y (2018) Plasmonic ELISA based on enzyme-assisted etching of Au nanorods for the highly sensitive detection of aflatoxin B1 in corn samples. *Sensors Actuators B Chem* 267:320–327. <https://doi.org/10.1016/j.snb.2018.04.027>
- Xu X, Ma X, Wang H, Wang Z (2018) Aptamer based SERS detection of *Salmonella typhimurium* using DNA-assembled gold nanodimers. *Microchim Acta* 185:325. <https://doi.org/10.1007/s00604-018-2852-0>
- Xue L, Zheng L, Zhang H, Jin X, Lin J (2018) An ultrasensitive fluorescent biosensor using high gradient magnetic separation and quantum dots for fast detection of foodborne pathogenic bacteria. *Sensors Actuators B Chem* 265:318–325. <https://doi.org/10.1016/j.snb.2018.03.014>
- Yadav A, Upadhyay Y, Bera RK, Sahoo SK (2020) Vitamin B6 cofactors guided highly selective fluorescent turn-on sensing of histamine using beta-cyclodextrin stabilized ZnO quantum dots. *Food Chem* 320:126611. <https://doi.org/10.1016/j.foodchem.2020.126611>
- Yaghubi F, Zeinoddini M, Saedinia AR, Azizi A, Samimi Nemati A (2020) Design of Localized Surface Plasmon Resonance (LSPR) biosensor for immunodiagnostic of *E. coli* O157:H7 using gold nanoparticles conjugated to the Chicken antibody. *Plasmonics* 15:1481–1487. <https://doi.org/10.1007/s11468-020-01162-2>
- Yang T, Cai F, Zhang X, Huang Y (2015) Nitrogen and sulfur codoped graphene quantum dots as a new fluorescent probe for Au³⁺ ions in aqueous media. *RSC Adv* 5:107340–107347. <https://doi.org/10.1039/c5ra20060a>
- Yang P, Zheng J, Xu Y, Zhang Q, Jiang L (2016) Colloidal synthesis and applications of plasmonic metal nanoparticles. *Adv Mater* 28:10508–10517. <https://doi.org/10.1002/adma.201601739>
- Yang S, Li Y, Wang S, Wang M, Chu M, Xia B (2018) Advances in the use of carbonaceous materials for the electrochemical determination of persistent organic pollutants. A review. *Microchim Acta* 185:112. <https://doi.org/10.1007/s00604-017-2638-9>
- Yi Y, Zeng W, Zhu G (2021) β -Cyclodextrin functionalized molybdenum disulfide quantum dots as nanoprobe for sensitive fluorescent detection of parathion-methyl. *Talanta* 222:121703. <https://doi.org/10.1016/j.talanta.2020.121703>
- Yin M, Wu C, Li H, Jia Z, Deng Q, Wang S, Zhang Y (2019) Simultaneous sensing of seven pathogenic bacteria by guanidine-functionalized upconversion fluorescent nanoparticles. *ACS Omega* 4:8953–8959. <https://doi.org/10.1021/acsomega.9b00775>
- Yola ML, Atar N (2017) Electrochemical detection of Atrazine by platinum nanoparticles/carbon nitride nanotubes with molecularly imprinted polymer. *Ind Eng Chem Res* 56:7631–7639. <https://doi.org/10.1021/acs.iecr.7b01379>
- You S-M, Luo K, Jung J-Y, Jeong K-B, Lee E-S, Oh M-H, Kim Y-R (2020) Gold nanoparticle-coated starch magnetic beads for the separation, concentration, and SERS-based detection of *E. coli* O157:H7. *ACS Appl Mater Interfaces* 12:18292–18300. <https://doi.org/10.1021/acsami.0c00418>

- Yüce M, Kurt H (2017) How to make nanobiosensors: surface modification and characterisation of nanomaterials for biosensing applications. *RSC Adv* 7:49386–49403. <https://doi.org/10.1039/c7ra10479k>
- Yüce M, Kurt H, Hussain B, Ow-Yang CW, Budak H (2018) Exploiting Stokes and anti-Stokes type emission profiles of aptamer-functionalized luminescent nanoprobes for multiplex sensing applications. *Chem Select* 3:5814–5823. <https://doi.org/10.1002/slct.201801008>
- Zhan S, Fang H, Fu J, Lai W, Leng Y, Huang X, Xiong Y (2019) Gold nanoflower-enhanced dynamic light scattering immunosensor for the ultrasensitive no-wash detection of *Escherichia coli* O157:H7 in milk. *J Agric Food Chem* 67:9104–9111. <https://doi.org/10.1021/acs.jafc.9b03400>
- Zhan C, Liu B-W, Tian Z-Q, Ren B (2020) Determining the interfacial refractive index via ultrasensitive plasmonic sensors. *J Am Chem Soc* 142:10905–10909. <https://doi.org/10.1021/jacs.0c01907>
- Zhang B, Li H, Pan W, Chen Q, Ouyang Q, Zhao J (2017) Dual-Color Upconversion Nanoparticles (UCNPs)-based fluorescent immunoassay probes for sensitive sensing foodborne pathogens. *Food Anal Methods* 10:2036–2045. <https://doi.org/10.1007/s12161-016-0758-1>
- Zhang A, Tao G, Wang J (2018) Assembly of bioconjugated rod-nanotags and multilayer plasmonic nanorod-array for ultrasensitive SERS detection of *S. aureus* bacteria. *J Nanopart Res* 20:97. <https://doi.org/10.1007/s11051-018-4200-z>
- Zhang D, Liu H, Geng W, Wang Y (2019a) A dual-function molecularly imprinted optopolymer based on quantum dots-grafted covalent-organic frameworks for the sensitive detection of tyramine in fermented meat products. *Food Chem* 277:639–645. <https://doi.org/10.1016/j.foodchem.2018.10.147>
- Zhang L, Yin S, Hou J, Zhang W, Huang H, Li Y, Yu C (2019b) Detection of choline and hydrogen peroxide in infant formula milk powder with near infrared upconverting luminescent nanoparticles. *Food Chem* 270:415–419. <https://doi.org/10.1016/j.foodchem.2018.07.128>
- Zhang B, Sheng W, Liu Y, Huang N, Zhang W, Wang S (2020a) Multiplexed fluorescence immunoassay combined with magnetic separation using upconversion nanoparticles as multi-color labels for the simultaneous detection of tyramine and histamine in food samples. *Anal Chim Acta* 1130:117–125. <https://doi.org/10.1016/j.aca.2020.07.043>
- Zhang S-W, Sun Y-Y, Sun Y-M, Wang H, Li Z-F, Xu Z-L (2020b) Visual upconversion nanoparticle-based immunochromatographic assay for the semi-quantitative detection of sibutramine. *Anal Bioanal Chem*. <https://doi.org/10.1007/s00216-020-02944-7>
- Zhao L, Wiebe J, Zahoor R, Slavkovic S, Malile B, Johnson PE, Chen JIL (2016) Colorimetric detection of catalase and catalase-positive bacteria (*E. coli*) using silver nanoprisms. *Anal Methods* 8:6625–6630. <https://doi.org/10.1039/C6AY01453D>
- Zhao F, Yao Y, Jiang C, Shao Y, Barceló D, Ying Y, Ping J (2020) Self-reduction bimetallic nanoparticles on ultrathin MXene nanosheets as functional platform for pesticide sensing. *J Hazard Mater* 384:121358. <https://doi.org/10.1016/j.jhazmat.2019.121358>
- Zheng L, Cai G, Wang S, Liao M, Li Y, Lin J (2019) A microfluidic colorimetric biosensor for rapid detection of *Escherichia coli* O157:H7 using gold nanoparticle aggregation and smart phone imaging. *Biosens Bioelectron* 124–125:143–149. <https://doi.org/10.1016/j.bios.2018.10.006>
- Zhou D, Wang M, Dong J, Ai S (2016) A novel electrochemical immunosensor based on mesoporous graphitic carbon nitride for detection of subgroup J of Avian leukosis viruses. *Electrochim Acta* 205:95–101. <https://doi.org/10.1016/j.electacta.2016.04.101>
- Zhou L, Zhang X, Ma L, Gao J, Jiang Y (2017) Acetylcholinesterase/chitosan-transition metal carbides nanocomposites-based biosensor for the organophosphate pesticides detection. *Biochem Eng J* 128:243–249. <https://doi.org/10.1016/j.bej.2017.10.008>

- Zhou C, Zou H, Li M, Sun C, Ren D, Li Y (2018) Fiber optic surface plasmon resonance sensor for detection of *E. coli* O157:H7 based on antimicrobial peptides and AgNPs-rGO. *Biosens Bioelectron* 117:347–353. <https://doi.org/10.1016/j.bios.2018.06.005>
- Zhou J, Ai R, Weng J, Li L, Zhou C, Ma A, Fu L, Wang Y (2020a) A “on-off-on” fluorescence aptasensor using carbon quantum dots and graphene oxide for ultrasensitive detection of the major shellfish allergen Arginine kinase. *Microchem J* 158:105171. <https://doi.org/10.1016/j.microc.2020.105171>
- Zhou S, Lu C, Li Y, Xue L, Zhao C, Tian G, Bao Y, Tang L, Lin J, Zheng J (2020b) Gold nanobones enhanced ultrasensitive surface-enhanced raman scattering aptasensor for detecting *Escherichia coli* O157:H7. *ACS Sensors* 5:588–596. <https://doi.org/10.1021/acssensors.9b02600>
- Zhu X, Liu P, Xue T, Ge Y, Ai S, Sheng Y, Wu R, Xu L, Tang K, Wen Y (2020) A novel graphene-like titanium carbide MXene/Au–Ag nanoshuttles bifunctional nanosensor for electrochemical and SERS intelligent analysis of ultra-trace carbendazim coupled with machine learning. *Ceram Int*. <https://doi.org/10.1016/j.ceramint.2020.08.121>